

L. PAJDUŠÁKOVÁ

THE ASYMMETRY OF THE SOLAR CORONA

Abstract: Investigated is the asymmetry of the solar corona in the green and red coronal line. The complete observational material was collected by nine leading corona stations (Alma Ata, Arosa, Climax, Kanzelhöhe, Kislovodsk, Norikura, Pic du Midi, Sacramento Peak, Wendelstein) from 1948 till 1961. The measurements show that the North-South asymmetry exists and that it corresponds to that of other phenomena on the Sun. The existence of the East-West asymmetry, however, was not borne out unambiguously. The discrepancies encountered result from great systematic errors in the determination of the coronal intensity due to varying atmospheric conditions combined with inadequate measuring methods. These errors are analysed in great detail according to their origin, and a method is devised to eliminate them. The East-West asymmetry — if any — is so slight that our present precision of determining the coronal intensities fails to prove it.

Introduction

Ever since discovered, the corona has shown an asymmetry in the sense that its intensity did not decrease uniformly in all directions from the solar limb. The shortlived and prolonged changes in its shape and area detected in due time, eventually led to the corona-asymmetry problem.

This asymmetry exists in the following three forms:

1. The flattening of the corona may be considered a “Pseudo-Asymmetry”. As early as in 1881, Ranyard and after him Hansky showed that this flattening undergoes changes as the 11-year cycle of solar activity wears on. With solar activity at minimum, the intensity of the corona decreases about the poles (polar flattening). The axis of symmetry of the flattening is identical with the Sun’s axis of rotation (Campbell, Moore and Baker 1923). In 1903, Lockyer found that the corona is related to prominences, whose frequency curve and curve of distribution over the solar surface do not square with the respective curves of spots. This coronal “pseudo-asymmetry” is borne out by ample observational material, especially on eclipses, and the problem of the corona flattening can be dismissed.

2. The North – South asymmetry (further on N – S asymmetry) was first discovered in spots and then also for other variable phenomena on the Sun. Even though some authors (e.g. Waldmeier) maintain that the changes in the distribution of the spots between the northern and southern hemisphere are definitely linked to both the 80- and 11-year cycle, the causes underlying them are not quite clear yet. Beside having been established from the material on eclipses, the N-S-type coronal asymmetry has not been dealt with in detail so far. We shall analyse it more closely, as we wish to compare it with the third type, the East-West asymmetry.

3. The East – West asymmetry (further on E – W asymmetry) was first mentioned by Mauder (1907), who had detected it in the area of spots and prominences. The results arrived at in more recent papers on this problem cannot be said fully to corroborate Mauder’s findings; they even contradict them. On materials covering several tens of years it was shown that there does not exist a preponderance of the eastern over the western half of the disc in the number and area of spots, as held by Mauder (Pocock 1919, Gleissberg 1947, Kulešová and Slonim 1957, Bruzek 1954, Kulešová 1963). The present paper is fully

devoted to the problem of the E – W corona asymmetry.

The authoress considers investigations into the coronal asymmetry useful, as they may add precision to what we know of the shape of the corona and its changes, and thus contribute to coronal studies in general. Moreover, the corona is the first medium sensitively to react upon the processes that take place in the lower layers of the Sun, so that coronal studies may add to a better understanding of the effects of solar activity upon processes on the Earth and its closest surroundings, or, as the case may be, of the reversed phenomenon, that is the effects of the planets on solar activity (Kopecký, Mayer 1951; Kopecký, Mayer, Borovičková 1952; Link 1964). In this respect, coronal studies are certain to be helpful in drafting forecasts.

Another asset of the present paper is its overall check-up on the quality of coronal observations, as made by stations that publish their results in the QBSA, and an evaluation of the factors that affect the homogeneity of coronal measurements.

The E – W asymmetry of the corona

1. Results achieved so far

The first to investigate the E – W asymmetry of the corona in more detail were Link and Linková (1956). Their results derived from the complete material, as published in the QBSA, were included in the last of a series of papers on the asymmetry of solar activity in general.

The authors studied the coronal asymmetry for the period from 1948 till 1953 in both the green 5303 Å and red 6374 Å emissions. As unit period they took the Sun's magnetic rotation. The period studied included 81 rotations, from No. 1902 to No. 1982. Their asymmetry indices were both the relative asymmetry expressed by formula $A = \frac{(E - W)}{(E + W)} \%$ and cumulative sums $\Sigma(E - W)$ of asymmetry for the magnetic rotations. Their papers included the number of rotations with positive and that of rotations with negative asymmetry as well as total asymmetry ($E - W$) all through the period from 1948 till 1953.

Link and Linková's results are roughly as follows:

1. The number of stations with recorded positive asymmetry in both the green and red line prevails

over that of stations with negative recordings.

2. The only striking exception, due—as the authors believe—to local conditions, is Arosa.

The authoress of the present paper carried the investigation into further two years, 1954 and 1955 (Pajdušáková 1957), thus adding 27 rotations, No. 1983 to 2009. It should be emphasized that this period coincided with a solar activity minimum. The results obtained by the method used by Link and Linková are not unambiguously in favour of the positive asymmetry. Only four out of ten cases showed a preponderance of the eastern over the western limb.

Owing to the fact that the extended series caused the character of cumulative sums ($E - W$) to change at some stations, which did not corroborate Link and Linková's results, and since the positive asymmetry of the spots was not unquestionable any longer, the authoress resolved to process the results of corona observations made in further six years, thus covering the period from 1956 till 1961 included (up to rotation No. 2089). This period coincided with the most active part of the high 19th cycle of solar activity.

2. Material and method of processing

The material processed in this paper includes observations made of the coronal intensity by 9 stations, whose results are published in the QBSA. Table I list the corona stations together with some further data.

The material was treated by the same method as in the foregoing papers (Link and Linková 1956, Pajdušáková 1957). First we had to add up the corona-intensity readings as obtained by 5° , separately for each of the four quadrants and for every day and station. E stands for the sum of the intensities from the North Pole— 0° —along the eastern limb of the disc to the South Pole— 180° —, in other words, for the total intensity of the corona in the Ist and IInd quadrant. W stands for the total intensity of the corona in the IIIrd and IVth quadrant, N for the sum of the intensities in the Ist and IVth quadrant and, eventually, S for the sum of the intensities in the IInd and IIIrd quadrant. The values at the critical position angles, that is 0° , 90° , 180° and 270° , were halved, and if uneven, the higher half was added to the following quadrant. Then:

$$(E + W) = (N + S) = \text{total intensity of corona},$$

$$(E - W) \text{ and } (N - S) = \text{total asymmetry of corona},$$

Table I
Coronal Stations

Station	Altitude in metres	Processed material		Number of rotations	Observational method
		from year	from rotation		
Arosa Kanzelhöhe Wendelstein	2200	1948	1902	188	visual estimates on 0 to 50 scale
	1900	1948	1904	186	
	1840	1948	1902	188	
Climax Sacramento Peak	3410	1948	1902	188	visual estimates on 0 to 40 scale, since 1959VI. photometric determination
	3550	1953	1969	121	
Alma Ata Kislovodsk Norikura Pic du Midi	2900	1958	2038	52	photometric determination
	2130	1957	2031	59	
	2900	1951	1943	147	
	2860	1948	1903	187	

$\frac{(E - W)}{(E + W)}$ and $\frac{(N - S)}{(N + S)}$ = relative asymmetry expressed in per cent,

$\Sigma(E - W)$ and $\Sigma(N - S)$ = cumulative sums of asymmetry for magnetic rotations.

3. Results and their discussion

The value of the total intensity of the corona, total asymmetry ($E - W$), relative asymmetry and cumulative sums $\Sigma(E - W)$ after the individual magnetic rotations for 9 stations from rotation No. 2010 through to rotation No. 2089 and for the emission in both the green and red line are listed in Table II.

Table II is completed by diagrams (Fig. 1 and 2) of cumulative sums $\Sigma(E - W)$, plotted from rotation No. 1902 onward.

The number of observational days, total intensity of the corona, final value of the cumulative sums and the final relative asymmetry for all rotations from No. 1902 to No. 2089 are listed in Table III.

The distribution of the relative asymmetry values is given in Table IV and Fig. 3.

The number of the observed rotations and the number of rotations with positive and negative asymmetry from rotation No. 1902 through to rotation No. 2089 are given in Table V.

The results listed in the tables for the period from 1948 till 1961 failed to corroborate the results of Link and Linková's paper (1956). Five out of the 9 stations show a negative final asymmetry in the green line, and hence only four stations are in

favour of the predominance of the eastern over the western limb. Similar is also the distribution of the number of the individual rotations with positive or negative asymmetry in the green line: Rotations with negative asymmetry prevail in 5 stations and only the 4 remaining ones show positive asymmetry.

Nor does the course of cumulative sums $\Sigma(E - W)$ substantiate the reality of positive asymmetry in the intensity of the corona (cf. Fig. 1.)

The conclusions arrived at from the course of the curves of the cumulative sums and by mutually comparing the stations that use similar observational methods are as follows:

a) A systematic rise in the curve of cumulative sums $\Sigma(E - W)$, that is systematic positive asymmetry, was only found for one station: Pic du Midi.

b) The overall tendency of this curve at the Norikura station is reversed to that of Pic du Midi, in other words, measurements made by the same method over the same period give an opposite result—negative asymmetry. At the Norikura station, cumulative sum $\Sigma(E - W)$ reached 8947 units since the results were begun to be published, that is from rotation No. 1943 through to rotation No. 2006, when its positive asymmetry was at peak, while the cumulative sum for Pic du Midi reached as much as 57599 units over the same period. From rotation No. 2006 until the end of the period in question the cumulative sum for Pic du Midi increased by further 158335 units, while that for Norikura went down by 119894 units. Thus, from rotation No. 2006 onwards, Pic du Midi and Norikura show an opposite

Table II
Green line — (5303 Å)

Alma Ata

Rot.	n	E + W	E - W	$\frac{E + W}{n}$	$\frac{E - W}{E + W}$	$\Sigma(E - W)$
2038	7	18775	-799	2682	-4.3	-799
2039	5	13032	-942	2606	-7.2	-1741
2040	2	6160	-1784	3080	-29.0	-3525
2041	—	—	—	—	—	-3525
2042	4	10585	-2283	2646	-21.6	-5808
2043	—	—	—	—	—	-5808
2044	—	—	—	—	—	-5808
2045	1	2200	-152	2200	-6.9	-5960
2046	12	36191	-2295	3016	-6.3	-8255
2047	9	22002	-2530	2445	-11.5	-10785
2048	7	19580	-2624	2797	-13.4	-13409
2049	11	27416	-3838	2492	-14.0	-17247
2050	4	9230	-1802	2307	-19.4	-19049
2051	10	25995	-1545	2599	-5.9	-20594
2052	6	18740	-1378	3123	-7.3	-21972
2053	7	12585	-891	1798	-7.1	-22863
2054	3	4885	-109	1628	-2.2	-22972
2055	6	8335	-233	1389	-2.8	-23205
2056	4	5730	+188	1432	+3.3	-23017
2057	2	5225	+689	2612	+3.2	-22328
2058	2	5888	+186	2944	+3.2	-22142
2059	5	22895	-2179	4579	-9.5	-24321
2060	1	2752	—78	2752	-2.8	-24399
2061	3	8747	-197	2916	-2.2	-24596
2062	2	9863	+319	4931	+3.2	-24277
2063	4	15197	-883	3799	-5.8	-25160
2064	4	13634	-524	3408	-3.8	-25684
2065	3	7045	+567	2348	+8.0	-25117
2066	4	12433	+1307	3108	+10.5	-23810
2067	7	23528	+138	3361	+0.6	-23672
2068	4	10446	+1864	2611	+17.8	-21808
2069	4	11150	-200	2787	-1.8	-22008
2070	3	7346	-530	2449	-7.2	-22538
2071	3	9139	+519	3046	+5.7	-22019
2072	11	25622	+238	2329	+0.9	-21781
2073	8	13334	+1152	1667	+8.6	-20629
2074	3	8608	+210	2869	+2.4	-20419
2075	4	7742	+1554	1935	+20.1	-18865
2076	5	12753	+3769	2551	+29.6	-15096
2077	6	13897	-583	2316	-4.2	-15679
2078	8	11223	-1025	1403	-9.1	-16704
2079	8	17670	-3578	2209	-20.2	-20282
2080	8	12948	+354	1618	+2.7	-19928
2081	3	3394	-66	1131	-1.9	-19994
2082	11	12262	-240	1115	-2.0	-20234
2083	4	6403	+647	1601	+10.1	-19587
2084	5	12350	+1590	2470	+12.9	-17997
2085	12	46490	-1280	3874	-2.7	-19277
2086	18	55971	-1287	3109	-2.3	-20564
2087	16	47913	-365	2995	-0.8	-20929
2088	12	26911	-865	4243	-3.2	-21784
2089	16	29803	-1859	1863	-6.2	-23643

Arosa

Rot.	n	E + W	E - W	$\frac{E + W}{n}$	$\frac{E - W}{E + W}$	$\Sigma(E - W)$
2010	7	5090	+860	727	+16.9	-6772
2011	—	—	—	—	—	-6772
2012	4	3852	+244	963	+6.3	-6528
2013	9	7748	+634	861	+8.2	-5894
2014	1	874	+150	874	+17.2	-5744
2015	3	2555	-483	852	-18.9	-6227
2016	1	788	+138	788	+17.7	-6089
2017	12	11580	-714	965	-6.2	-6803
2018	18	18700	+984	1039	+5.3	-5819

Rot.	n	E + W	E - W	$\frac{E + W}{n}$	$\frac{E - W}{E + W}$	$\Sigma(E - W)$
2019	13	13279	+9	1056	+0.1	-5810
2020	2	2552	+108	1276	+8.2	-5702
2021	—	—	—	—	—	-5702
2022	—	—	—	—	—	-5702
2023	3	3023	+37	1008	+1.2	-5665
2024	—	—	—	—	—	-5665
2025	1	1129	-63	1129	-5.6	-5728
2026	14	18438	+272	1317	+1.5	-5456
2027	9	11719	+185	1302	+1.6	-5271
2028	2	2296	+272	1148	+11.8	-4999
2029	3	3602	+178	1201	+4.9	-4821
2030	3	3819	+175	1273	+4.6	-4646
2031	5	6625	-25	1325	-0.4	-4671
2032	—	—	—	—	—	-4671
2033	3	4060	-190	1353	-5.1	-4861
2034	7	10356	+1514	1479	+14.6	-3347
2035	—	—	—	—	—	-3347
2036	2	2775	+167	1388	+6.0	-3180
2037	7	10184	-162	1455	-1.6	-3342
2038	—	—	—	—	—	-3342
2039	4	5779	-503	1445	-8.7	-3845
2040	10	12247	-115	1225	-0.9	-3960
2041	2	2664	-84	1332	-3.2	-4044
2042	2	2069	+7	1035	+0.3	-4037
2043	1	1136	-46	1136	-4.0	-4083
2044	8	10025	-321	1253	-3.2	-4404
2045	11	14297	-495	1300	-3.5	-4899
2046	2	2800	+96	1400	+3.4	-4803
2047	—	—	—	—	—	-4803
2048	1	1096	-110	1096	-10.0	-4913
2049	—	—	—	—	—	-4913
2050	3	2940	+136	980	+4.6	-4777
2051	—	—	—	—	—	-4777
2052	3	4058	+48	1353	+1.2	-4729
2053	9	10771	-273	1197	-2.5	-5002
2054	9	10109	+227	1123	+2.2	-4775
2055	—	—	—	—	—	-4775
2056	1	1053	-19	1053	-1.8	-4794
2057	4	4070	+52	1018	+1.3	-4772
2058	—	—	—	—	—	-4772
2059	16	18274	+618	1142	+3.4	-4124
2060	7	9090	-1140	1299	-12.5	-5264
2061	4	4801	+359	1200	+7.5	-4905
2062	—	—	—	—	—	-4905
2063	—	—	—	—	—	-4905
2064	4	3228	+236	807	+7.2	-4669
2065	—	—	—	—	—	-4669
2066	2	1667	-231	834	-13.8	-4900
2067	13	11557	+139	889	+1.2	-4761
2068	2	1789	+59	895	+3.3	-4702
2069	—	—	—	—	—	-4702
2070	2	1474	+292	737	+19.8	-4410
2071	—	—	—	—	—	-4410
2072	8	6279	-59	785	-0.9	-4469
2073	5	4117	-817	823	-19.8	-5286
2074	6	5938	+580	990	+9.8	-4706
2075	—	—	—	—	—	-4706
2076	—	—	—	—	—	-4706
2077	6	4354	+1008	726	+23.2	-3698
2078	1	1037	-61	1037	-5.9	-3759
2079	—	—	—	—	—	-3759
2080	18	13771	+417	765	+3.0	-3342
2081	7	5610	-524	801	-9.3	-3866
2082	—	—	—	—	—	-3866
2083	—	—	—	—	—	-3866
2084	6	4088	+156	681	+3.8	-3710
2085	7	4364	-590	623	-13.5	-4300
2086	—	—	—	—	—	-4300
2087	4	2103	-17	526	-0.8	-4317
2088	7	5361	-465	766	-8.7	-4782
2089	—	—	—	—	—	-4782

Continuation Table II

Climax						
Rot.	n	E + W	E - W	E + W n	E - W E + W	$\Sigma(E - W)$
2010	9	16581	-473	1842	-2.8	+8
2011	4	8637	+153	2159	+1.8	+161
2012	8	18226	+468	2278	+2.6	+629
2013	16	37006	+512	2313	+1.4	+1141
2014	12	29616	-1324	2468	-4.5	-183
2015	14	35488	-608	2535	-1.7	-791
2016	18	47535	+389	2641	+0.8	-402
2017	24	81001	-429	3375	-0.5	-831
2018	20	73855	+59	3693	+0.1	-772
2019	24	85477	+2037	3562	+2.4	+1265
2020	21	78812	-1268	3753	-1.6	-3
2021	13	57690	-1802	4438	-3.1	-1805
2022	16	68953	+1493	4310	+2.2	-312
2023	15	72087	-2403	4806	-3.3	-2715
2024	4	15390	+1432	3848	+9.3	-1283
2025	3	10775	+13	3592	+0.1	-1270
2026	5	22977	+421	4595	+1.8	-849
2027	5	24957	-323	4991	-1.3	-1172
2028	9	39508	+708	4390	+1.8	-464
2029	13	62770	-932	5267	-1.5	-1396
2030	15	72471	-1215	4831	-1.7	-2611
2031	14	66218	+2086	4730	+3.2	-525
2032	16	78149	+4205	4884	+5.4	+3680
2033	16	72862	+992	4554	+1.4	+4672
2034	9	52178	+3324	5798	+6.4	+7996
2035	19	87890	-714	4626	-0.8	+7282
2036	17	73961	+5299	4350	+7.2	+12581
2037	14	67938	+2202	4853	+3.2	+14783
2038	4	17676	-2950	4419	-16.7	+11833
2039	8	26310	+2582	3289	+9.8	+14415
2040	4	17710	-130	4428	-0.7	+14285
2041	9	37696	+1518	4188	+4.0	+15803
2042	9	37662	+3882	4185	+10.3	+19685
2043	8	40212	-358	5026	-0.9	+19327
2044	11	44641	+387	4058	+0.9	+19714
2045	17	86425	-5659	5084	-6.6	+14055
2046	15	66399	-1793	4427	-2.7	+12262
2047	17	70241	+1283	4132	+1.8	+13545
2048	11	44861	-1019	4078	-2.3	+12526
2049	11	46732	+2346	4248	+5.0	+14872
2050	6	27802	+8	4633	+0.0	+14880
2051	4	18264	-434	4566	-2.4	+14446
2052	2	7923	-1029	3962	-13.0	+13417
2053	4	18608	-306	4652	-1.6	+13111
2054	5	21165	-1049	4233	-5.0	+12062
2055	—	—	—	—	+12062	
2056	12	40369	+101	3364	+0.2	+12163
2057	4	14768	+70	3692	+0.5	+12223
2058	10	42688	+3294	4269	+7.7	+15527
2059	15	71633	+817	4776	+1.1	+16344
2060	4	15717	-529	3929	-3.4	+15815
2061	13	44362	+1816	3412	+4.1	+17631
2062	13	39268	-784	3021	+2.0	+18415
2063	13	42931	-555	3302	-1.3	+17860
2064	4	12462	-220	3116	-1.8	+17640
2065	1	2735	-989	2735	+36.2	+18629
2066	2	3923	+327	1962	+8.3	+18956
2067	10	22515	+543	2252	+2.4	+19499
2068	11	22079	+11165	2007	+5.3	+20664
2069	10	18181	-921	1818	-5.1	+19743
2070	17	39605	+1959	2330	+4.9	+21702
2071	16	40561	+661	2535	+1.6	+22363
2072	20	43026	+2390	2151	+5.5	+24753
2073	19	45863	+3911	2414	+8.5	+28664
2074	13	28570	-1580	2198	-5.5	+27084
2075	11	23217	+1773	2111	+7.6	+28857
2076	14	26171	+1975	1869	+7.5	+30832
2077	11	20171	+2357	1834	+11.7	+33189
2078	18	30220	-2080	1679	-6.9	+31109
2079	6	10784	+126	1797	+1.2	+31235
2080	5	6298	-44	1260	-0.7	+31191

Rot.	n	E + W	E - W	E + W n	E - W E + W	$\Sigma(E - W)$
2081	3	3352	-736	1117	-21.9	+30455
2082	4	6026	-350	1506	-5.8	+30105
2083	7	9611	+1995	1373	+20.7	+32100
2084	13	22069	+3627	1698	+14.8	+35727
2085	5	8261	+1549	1652	+18.7	+37276
2086	11	17606	-2988	1600	-17.0	+34288
2087	17	23852	+1658	1403	+6.9	+35946
2088	15	22691	-37	1513	-0.2	+35909
2089	11	16507	-551	1501	-3.3	+35558

Kanzelhöhe

Rot.	n	E + W	E - W	E + W n	E - W E + W	$\Sigma(E - W)$
2010	8	3467	+75	433	+2.2	+342
2011	5	2053	+17	411	+0.8	+359
2012	12	8066	-1068	672	-13.2	-709
2013	1	697	-21	697	-3.0	-730
2014	2	1453	+293	727	+19.0	-437
2015	5	3106	+360	621	+11.6	-77
2016	2	1609	+329	805	+20.4	+252
2017	7	5595	+7	799	+0.1	+259
2018	13	10091	+305	776	+3.0	+564
2019	12	10149	-489	846	-4.8	+75
2020	11	13691	+261	1245	+1.9	+336
2021	12	14259	-639	1188	-4.5	-303
2022	4	4091	+235	1023	+5.7	-68
2023	10	10592	-380	1059	-3.6	-448
2024	10	11227	+487	1123	+4.3	+39
2025	6	4932	-338	822	-6.8	-299
2026	12	9642	-410	804	-4.2	-709
2027	6	4866	-164	811	-3.4	-873
2028	12	10526	-166	877	-1.6	-1039
2029	7	9308	+406	1330	+4.4	-633
2030	18	19783	-435	1099	-2.2	-1068
2031	12	13020	-356	1085	-2.7	-1424
2032	11	10596	+1074	963	+10.1	-350
2033	9	9737	+155	1082	+1.6	-195
2034	19	24471	-631	1288	-2.6	-826
2035	9	11537	-251	1282	-2.2	-1077
2036	13	16400	+1164	1262	+7.1	+87
2037	12	13936	-672	1161	-4.8	-585
2038	9	9711	-361	1079	-3.7	-946
2039	7	5820	-136	831	-2.3	-1082
2040	10	10873	-1389	1087	-12.8	-2471
2041	13	12171	+77	936	+0.6	-2394
2042	15	10453	-151	697	-1.4	-2545
2043	8	8590	-132	1074	-1.5	-2677
2044	20	20008	-770	1000	-3.8	-3447
2045	21	27991	+241	1333	+0.9	-3206
2046	19	19668	+582	1035	+3.0	-2624
2047	11	12132	+278	1103	+2.3	-2346
2048	11	16501	+841	1500	+5.1	-1505
2049	12	15749	+569	1312	+3.6	-936
2050	5	5625	+335	1125	+6.0	-601
2051	15	15977	-605	1065	-3.8	-1206
2052	22	25961	-73	1180	-0.3	-1279
2053	9	7699	+3	855	+0.0	-1276
2054	17	11609	-59	683	-0.5	-1335
2055	11	9942	+284	904	+2.9	-1051
2056	9	5848	+238	650	+4.1	-813
2057	12	11708	+518	976	+4.4	-295
2058	10	10154	+486	1015	+4.8	+191
2059	8	7901	-1369	988	-17.3	-1178
2060	18	16089	-1191	894	-7.4	-2369
2061	17	17371	+27	1022	+0.2	-2342
2062	6	5830	+298	972	+5.1	-2044
2063	7	5116	-556	731	-0.9	-2600
2064	6	5408	-40	901	-0.7	-2640
2065	8	7102	-276	888	-3.9	-2916

Continuation Table II

Rot.	n	E + W	E - W	$\frac{E + W}{n}$	$\frac{E - W}{E + W}$	$\Sigma(E - W)$	Rot.	n	E + W	E - W	$\frac{E + W}{n}$	$\frac{E - W}{E + W}$	$\Sigma(E - W)$
2066	6	4814	+166	802	+3.4	-2750	2070	13	43171	+4555	3321	+10.5	+3329
2067	4	3121	-221	780	-7.1	-2971	2071	15	48935	+4525	3262	+9.2	+7854
2068	6	4767	-169	795	-3.5	-3140	2072	16	54938	+3498	3434	+6.4	+11352
2069	6	5129	+205	855	+4.0	-2935	2073	17	58878	+3038	3463	+5.2	+14390
2070	9	7311	-257	812	-3.5	-3192	2074	17	56873	+7295	3345	+12.8	+21685
2071	10	10313	-381	1031	-3.7	-3573	2075	14	38711	+3429	2765	+8.9	+25114
2072	9	8039	+269	893	+3.3	-3304	2076	10	26684	-1938	2668	-7.3	+23176
2073	14	12192	-384	871	-3.1	-3688	2077	13	35248	+1438	2711	+4.1	+24614
2074	3	3070	+56	1023	+1.8	-3632	2078	12	25893	+411	2158	+1.6	+25025
2075	2	1941	+229	971	+11.8	-3403	2079	11	23899	+4775	2173	+20.0	+29800
2076	9	7958	+298	884	+3.7	-3105	2080	2	6370	-428	3185	-6.7	+29372
2077	2	1606	+482	803	+30.0	-2623	2081	11	20490	-524	1863	-2.6	+28848
2078	9	8347	+605	927	+7.2	-2018	2082	8	13039	+1505	1630	+11.5	+30353
2079	13	10691	+557	822	+5.2	-1461	2083	8	18759	+1771	2345	+9.4	+32124
2080	10	7676	+1228	768	+16.0	-233	2084	5	10323	+191	2065	+1.8	+32315
2081	4	3157	-17	789	-0.5	-250	2085	13	24171	+2147	1859	+8.9	+34462
2082	1	601	-13	601	-2.2	-263	2086	16	43101	+3439	2694	+8.0	+37901
2083	1	1358	-236	1358	-17.4	-499	2087	18	39484	+5698	2194	+14.4	+43599
2084	2	1105	-89	553	-8.0	-588	2088	13	20943	+1665	1611	+7.9	+45264
2085	10	5793	+609	579	+10.5	+21	2089	7	12084	+844	1726	+7.0	+46108
2086	11	6325	-47	575	-0.7	-26							
2087	18	11315	-501	629	-4.4	-527							
2088	4	2491	+105	623	+4.2	-422							
2089	3	1793	+381	598	+21.2	-41							

Norikura

Rot.	n	E + W	E - W	$\frac{E + W}{n}$	$\frac{E - W}{E + W}$	$\Sigma(E - W)$	Rot.	n	E + W	E - W	$\frac{E + W}{n}$	$\frac{E - W}{E + W}$	$\Sigma(E - W)$
2031	19	61235	+4683	3223	+7.6	+4683	2010	3	7912	+326	2637	+4.1	+3988
2032	18	65479	+6673	3638	+10.2	+11356	2011	1	4625	+387	4625	+8.4	+4375
2033	16	64873	+2379	4055	+3.7	+13735	2012	3	3546	+546	1182	+15.4	+4921
2034	19	76121	+4585	4006	+6.6	+18320	2013	4	16615	+119	4154	+0.7	+5040
2035	17	66374	+3552	3904	+5.3	+21872	2014	7	20131	-871	2876	-4.3	+4169
2036	6	18218	-1032	3036	-5.7	+20840	2015	4	10779	+491	2695	+4.6	+4660
2037	7	25481	-1897	3640	-7.4	+18943	2016	2	7149	+253	3575	+3.5	+4913
2038	8	23938	-564	2992	-2.3	+18379	2017	6	28496	-6782	4749	-23.8	-1869
2039	7	17399	+75	2486	+0.4	+18454	2018	13	68202	-2914	5246	-4.3	-4783
2040	7	17782	+322	2540	+1.8	+18776	2019	7	36074	-5606	5153	-15.5	-10389
2041	10	27242	-444	2724	-1.6	+18332	2020	4	18331	-5227	4583	-28.5	-15616
2042	13	38249	+47	2942	+0.1	+18379	2021	6	27200	-4462	4533	-16.4	-20078
2043	12	40205	+2241	3350	+5.6	+20620	2022	8	42014	-4638	5252	-11.0	-24716
2044	13	42234	-858	3249	-2.0	+19762	2023	4	15073	-2547	3768	-16.9	-27263
2045	18	56891	-3085	3161	-5.4	+16677	2024	5	24996	-808	4999	-3.2	-28071
2046	13	43209	-1399	3324	-3.2	+15278	2025	—	—	—	—	—	-28071
2047	19	60596	-780	3180	-1.3	+14498	2026	4	16103	-2667	4026	-16.6	-30738
2048	16	54838	-3866	3427	-7.0	+10632	2027	10	35960	-6024	3596	-16.8	-36762
2049	12	34930	-1418	2911	-4.0	+9214	2028	6	19961	-5911	3327	-29.6	-42673
2050	11	36363	-1615	3306	-4.4	+7599	2029	5	20495	-1509	4099	-7.4	-44182
2051	7	22618	+270	3231	+1.2	+7869	2030	2	9377	-1763	4689	-18.8	-45945
2052	7	20582	+92	2940	+0.4	+7961	2031	5	14783	-347	2957	-2.4	-46292
2053	12	36373	-1111	3031	-3.0	+6850	2032	2	8055	+1221	4028	+15.2	-45071
2054	15	53673	+2891	3578	+5.4	+9741	2033	3	11798	-2884	3933	-24.4	-47955
2055	3	10956	-170	3652	-1.5	+9571	2034	12	44837	+1199	3736	+2.7	-46756
2056	10	37033	-667	3703	-1.8	+8904	2035	17	78272	-9502	4604	-12.1	-56258
2057	13	39186	-148	3014	-0.4	+8756	2036	8	44508	-5032	5564	-11.3	-61290
2058	12	40312	-58	3359	-0.1	+8698	2037	2	12315	-97	6157	-0.7	-61387
2059	19	74337	-3697	3912	-5.0	+5001	2038	1	3017	+25	3017	+0.8	-61362
2060	10	37671	-1827	3767	-4.8	+3174	2039	6	25107	-3232	4185	-13.2	-64685
2061	12	42786	-1556	3566	-3.6	+1618	2040	4	15583	+63	3896	+0.4	-64622
2062	6	19365	-761	3228	-3.9	+857	2041	6	17618	-5048	2936	-28.6	-69670
2063	7	22593	-2141	3228	-9.5	-1284	2042	5	11957	-665	2391	-5.6	-70335
2064	8	29337	-277	3667	-0.9	-1561	2043	4	20949	-1293	5237	-6.2	-71628
2065	6	26116	-2204	4353	-8.4	-3765	2044	2	4677	-1763	2339	-37.7	-73391
2066	5	17229	+371	3446	+2.2	-3394	2045	1	2749	-7	2749	-0.3	-73398
2067	11	33130	+1388	3012	+4.2	-2006	2046	5	18871	+951	3774	+5.0	-72447
2068	5	16686	+1776	3337	+10.6	-230	2047	7	23737	+6011	3391	+25.3	-66436
2069	7	23596	-996	3371	-4.2	-1226	2048	5	24665	-2497	4933	-10.1	-68933
							2049	11	45325	+1105	4120	+2.4	-67828
							2050	5	11280	+220	2256	+2.0	-67608
							2051	3	7296	-2980	2432	-40.8	-70588
							2052	5	6986	-550	1397	-7.9	-71138

Continuation Table II

Rot.	n	E + W	E - W	$\frac{E + W}{n}$	$\frac{E - W}{E + W}$	$\Sigma(E - W)$	Rot.	n	E + W	E - W	$\frac{E + W}{n}$	$\frac{E - W}{E + W}$	$\Sigma(E - W)$
2053	6	12918	-1666	2153	-12.9	-72804	2037	10	42077	+4675	4207	+11.1	+171783
2054	6	11021	-601	1834	-5.4	-73405	2038	11	39007	+4459	3546	+11.4	+176242
2055	4	6409	-1609	1602	-25.1	-75014	2039	4	13607	+1205	3402	+8.9	+177447
2056	5	15102	-1234	3020	-8.2	-76248	2040	2	6544	-654	3272	-10.0	+176793
2057	4	12403	-1093	3101	-8.8	-77341	2041	7	19487	+2205	2784	+11.3	+178998
2058	14	36855	+7641	2633	+20.7	-69700	2042	4	11544	+2118	2886	+18.4	+181116
2059	7	14115	+555	2016	+3.9	-69145	2043	6	17338	+1266	2890	+7.3	+182382
2060	5	14172	-1944	2834	-13.7	-71089	2044	17	40550	+4102	2385	+10.1	+186484
2061	8	20731	+249	2591	+1.2	-70840	2045	13	35800	-1006	2754	+2.8	+185478
2062	8	22534	-1258	2817	-5.6	-72098	2046	13	40513	+4737	3116	+11.7	+190215
2063	8	28214	-4590	3527	-16.3	-76688	2047	12	40112	+3716	3343	+9.3	+193931
2064	5	15765	-3147	3153	-20.0	-79835	2048	11	38479	+1883	3498	+4.9	+195814
2065	3	9447	-2455	3149	-26.0	-82290	2049	5	16922	+1930	3384	+8.2	+197204
2066	7	24855	-4827	3551	-19.4	-87117	2050	4	12631	+2235	3158	+17.7	+199439
2067	5	15774	-1110	3155	-7.0	-88227	2051	9	27950	+2770	3106	+9.9	+202209
2068	5	21589	-1647	4318	-7.6	-89874	2052	16	39789	+2919	2487	+7.3	+205128
2069	4	12459	-4161	3115	-33.4	-94035	2053	7	23032	+1056	3290	+4.6	+206184
2070	2	4338	-256	2169	-5.9	-94291	2054	6	16417	-145	2736	-0.9	+206039
2071	5	14598	+672	2920	+4.6	-93619	2055	6	21761	+3569	3627	+16.4	+209608
2072	10	30588	-2334	3059	-7.6	-95953	2056	13	35646	+5986	2742	+16.8	+215594
2073	3	8002	-1288	2667	-16.1	-97241	2057	12	35069	+2835	2922	+8.1	+218429
2074	7	17396	-1608	2485	-9.2	-98849	2058	15	38802	+1924	2587	+5.0	+220353
2075	13	35613	-5929	2739	-16.6	-104778	2059	7	15614	+824	2231	+5.3	+221177
2076	8	22601	-3141	2825	-13.9	-107919	2060	2	6916	-42	3458	-0.6	+221135
2077	—	—	—	—	—	-107919	2061	10	26073	+2949	2607	+11.3	+224084
2078	2	5651	+1691	2825	+29.9	-106228	2062	9	26037	-649	2843	-2.5	+223435
2079	—	—	—	—	—	-106228	2063	6	18524	+910	3087	+4.9	+224345
2080	6	10447	+477	1741	+4.6	-105751	2064	7	17868	+1732	2553	+9.7	+226077
2081	2	3257	-777	1628	-23.9	-106528	2065	7	19675	+399	2811	+2.0	+226476
2082	4	7027	+251	1758	+3.6	-106277	2066	6	17213	+565	2869	+3.3	+227041
2083	3	6415	-593	2135	-9.2	-106870	2067	3	7995	+773	2665	+9.7	+227814
2084	2	5453	+859	2726	+15.7	-106011	2068	10	38805	+743	3881	+1.9	+228557
2085	—	—	—	—	—	-106011	2069	6	23922	+26	3987	+0.1	+228583
2086	—	—	—	—	—	-106011	2070	9	33899	-1583	3767	-4.7	+227000
2087	—	—	—	—	—	-106011	2071	11	32654	+356	2969	+1.1	+227356
2088	—	—	—	—	—	-106011	2072	11	29169	+2133	2652	+7.3	+229489
2089	4	3538	-220	884	-6.2	-106231	2073	14	46970	+3208	3355	+6.8	+232697

Pic du Midi

Rot.	n	E + W	E - W	$\frac{E + W}{n}$	$\frac{E - W}{E + W}$	$\Sigma(E - W)$
2010	6	12841	+1617	2140	+12.6	+100083
2011	9	19461	+4001	2162	+20.6	+104084
2012	16	40666	+5236	2542	+12.9	+109320
2013	9	24949	+3857	2772	+15.5	+113177
2014	6	18949	+3587	3158	+18.9	+116764
2015	12	35272	+5472	2939	+15.5	+122236
2016	11	29958	+4272	2723	+14.3	+126508
2017	15	43066	+1086	2871	+2.5	+127594
2018	25	67771	+3677	2711	+5.4	+131271
2019	17	62103	+8171	3653	+13.2	+139442
2020	12	45082	+2880	3757	+6.4	+142322
2021	9	33317	+3233	3702	+9.7	+145555
2022	13	50537	+4693	3887	+9.3	+150248
2023	5	15840	+1574	3168	+9.9	+151822
2024	13	48924	+7080	3764	+14.5	+158902
2025	6	24679	+1577	4113	+6.4	+160479
2026	8	32325	+2827	4041	+8.8	+163306
2027	8	31566	-956	3946	-3.0	+162350
2028	5	17994	+1066	3599	+5.9	+163416
2029	5	18157	+1511	3631	+8.3	+164927
2030	7	29056	-1902	4151	-6.6	+163025
2031	12	42378	-54	3531	-0.1	+162971
2032	21	72731	-4293	3463	-5.9	+158678
2033	5	20253	+85	4051	+0.4	+158763
2034	14	54995	+3125	3982	+5.7	+161888
2035	10	39410	+432	3941	+1.1	+162320
2036	15	54514	+4788	3634	+8.8	+167108

Sacramento peak

Rot.	n	E + W	E - W	$\frac{E + W}{n}$	$\frac{E - W}{E + W}$	$\Sigma(E - W)$
2010	12	11427	+1183	952	+10.4	-222
2011	6	5720	+350	953	+6.1	+128
2012	16	18274	-32	1142	-0.2	+96
2013	15	22831	+707	1522	+3.1	+803
2014	15	28221	+727	1881	+2.6	+1530
2015	12	21619	-839	1802	-3.9	+691
2016	2	3393	+285	1697	+8.4	+976
2017	5	7423	+167	1485	+2.2	+1143
2018	25	19194	-1486	768	-7.7	-343
2019	14	36349	+263	2596	+0.7	-80
2020	18	39401	-2217	2189	-5.6	-2297

Continuation Table 11

Wendelstein							
Rot.	n	E + W	E - W	$\frac{E + W}{n}$	$\frac{E - W}{E + W}$	$\Sigma(E - W)$	
2021	21	61805	-4045	2943	-6.5	-6342	
2022	17	53964	-326	3174	-0.6	-6668	
2023	16	51037	+115	3190	+0.2	-6553	
2024	7	19404	-596	2772	-3.1	-7149	
2025	11	34917	-2011	3174	-5.8	-9160	
2026	11	29959	+243	2724	+0.8	-8917	
2027	13	34659	-1463	2666	-4.2	-10380	
2028	12	32723	+453	2727	+1.4	-9927	
2029	18	61482	-1706	3416	-2.8	-11633	
2030	2	5498	-1092	2749	-19.9	-12725	
2031	—	—	—	—	—	-12725	
2032	—	—	—	—	—	-12725	
2033	—	—	—	—	—	-12725	
2034	—	—	—	—	—	-12725	
2035	—	—	—	—	—	-12725	
2036	—	—	—	—	—	-12725	
2037	6	23734	-106	3956	-0.4	-12831	
2038	3	15823	-1459	5274	-9.2	-14290	
2039	4	14013	-1883	3503	-13.4	-16173	
2040	7	33202	+1176	4743	+3.5	-14997	
2041	8	39409	-75	4926	-0.2	-15072	
2042	6	23903	-159	3984	-0.7	-15231	
2043	8	38304	+3358	4788	+8.8	-11873	
2044	7	33081	-2113	4726	-6.4	-13986	
2045	—	—	—	—	—	-13986	
2046	3	13667	-829	4556	-6.1	-14815	
2047	6	28236	-104	4706	-0.4	-14919	
2048	10	49124	+556	4912	+1.1	-14363	
2049	4	20300	+476	5075	+2.3	-13887	
2050	14	57296	+824	4093	+1.4	-13063	
2051	10	37197	+25	3720	+0.1	-13038	
2052	12	47695	+639	3975	+1.3	-12399	
2053	6	21851	+579	3642	+2.6	-11820	
2054	8	30142	-882	3768	-2.9	-12702	
2055	8	29236	+1704	3655	+5.8	-10988	
2056	8	30692	-788	3837	-2.6	-11786	
2057	3	14226	+1260	4742	+8.9	-10526	
2058	5	18759	+2375	3752	+12.7	-8151	
2059	4	13924	+432	3481	+3.1	-7719	
2060	13	52769	-910	4048	-1.7	-8629	
2061	2	7133	+469	3567	+6.6	-8160	
2062	9	31666	+1358	3518	+4.3	-6802	
2063	3	11311	-1615	3770	-14.3	-8417	
2064	4	8149	-933	2037	-11.4	-9350	
2065	4	8747	+1177	2187	+13.4	-8173	
2066	3	6273	+603	2091	+9.6	-7570	
2067	4	5248	+194	1312	+3.7	-7376	
2068	—	—	—	—	—	-7376	
2069	5	7772	+302	1554	+3.9	-7074	
2070	3	4218	+910	1406	+21.4	-6164	
2071	2	3484	-306	1472	-8.8	-6470	
2072	4	8056	+1410	2014	+17.5	-5060	
2073	5	10245	+707	2049	+6.9	-4353	
2074	8	16653	-831	2082	-5.0	-5184	
2075	8	12437	+1545	1555	+12.4	-3639	
2076	4	6181	+325	1545	+5.2	-3314	
2077	7	8963	+87	1280	+1.0	-3227	
2078	1	1198	-38	1198	-3.2	-3265	
2079	9	11151	+2895	1239	+26.0	-370	
2080	7	8876	+1412	1268	+15.9	+1042	
2081	10	13621	+933	1362	+6.8	+1975	
2082	5	6749	-345	1350	-5.1	-1630	
2083	3	4984	+224	1661	+4.5	-1854	
2084	1	1543	-189	1543	-12.2	-1665	
2085	7	6740	+456	9629	+6.8	-2121	
2086	4	4925	-35	1231	-0.7	-2086	
2087	5	4262	-184	852	-4.3	-1902	
2088	15	4299	+615	287	+14.3	-2517	
2089	11	4640	-1082	422	-23.3	-1435	
Rot.	n	E + W	E - W	$\frac{E + W}{n}$	$\frac{E - W}{E + W}$	$\Sigma(E - W)$	
2010	3	1790	-70	597	-3.9	+15976	
2011	2	959	-15	480	-1.6	+15961	
2012	6	4220	-618	703	-14.6	+15343	
2013	7	4538	+78	648	+1.7	+15421	
2014	3	2313	+109	771	+4.7	+15530	
2015	8	7633	-683	954	-9.0	+14847	
2016	3	3421	+887	1140	+25.9	+15734	
2017	14	15916	+1498	1137	+9.4	+17232	
2018	14	16276	-472	1163	-2.9	+16760	
2019	13	15745	-791	1211	-5.0	+15969	
2020	17	25978	-1764	1528	-6.8	+14205	
2021	9	16273	-695	1808	-4.3	+13510	
2022	10	15709	+681	1571	+4.3	+14191	
2023	7	13284	-382	1898	-2.9	+13809	
2024	11	20325	+363	1848	+1.8	+14172	
2025	6	16213	-85	2102	-0.7	+14087	
2026	9	16857	-13	1873	-0.1	+14074	
2027	8	13713	+71	1714	+0.5	+14145	
2028	6	10112	+198	1685	+2.0	+14343	
2029	11	15474	+1074	1407	+6.9	+15417	
2030	13	19873	+1037	1529	+5.2	+18454	
2031	7	10291	+589	1470	+5.7	+17043	
2032	4	7807	-387	1952	-5.0	+16656	
2033	8	14209	-907	1776	-6.4	+15749	
2034	20	40367	+427	2018	+1.1	+16176	
2035	14	29707	-1059	2122	-3.6	+15117	
2036	8	14903	-501	1863	-3.4	+14616	
2037	6	9601	+7	1600	+0.1	+14623	
2038	8	11193	+167	1399	+1.5	+14790	
2039	3	3683	+47	1228	+1.3	+14837	
2040	9	11042	-224	1227	-2.0	+14613	
2041	7	10124	-746	1446	-7.4	+13867	
2042	4	5740	+18	1435	+0.3	+13885	
2043	4	6912	+446	1728	+6.4	+14331	
2044	12	21847	-1673	1821	-7.7	+12658	
2045	15	25371	+475	1691	+1.9	+13133	
2046	15	24312	-242	1621	-1.0	+12891	
2047	5	8846	-94	1769	-1.1	+12797	
2048	11	21183	-241	1926	-1.1	+12556	
2049	11	20786	-118	1890	-0.6	+12438	
2050	8	15561	+29	1945	+0.2	+12467	
2051	7	12951	+865	1850	+6.7	+13332	
2052	22	39772	-586	1808	-1.5	+12746	
2053	9	17353	-721	1928	-4.2	+12025	
2054	9	17171	+41	1908	+0.2	+12066	
2055	8	12092	+42	1512	+0.4	+12108	
2056	5	7474	-132	1495	-1.8	+11976	
2057	11	15607	-351	1419	-2.2	+11625	
2058	7	12483	-489	1783	-3.9	+11136	
2059	15	27854	-1836	1857	-6.6	+9300	
2060	16	26113	-839	1632	-3.2	+8461	
2061	15	25814	-1724	1721	-6.7	+6737	
2062	10	13604	+162	1360	+1.2	+6899	
2063	11	15894	-1428	1445	-9.0	+5471	
2064	5	6092	+70	1218	+1.2	+5841	
2065	10	13196	-130	1320	-1.0	+5411	
2066	4	5473	+1	1368	+0.0	+5412	
2067	9	11817	+931	1313	+7.9	+6343	
2068	4	5020	-218	1255	-4.3	+6125	
2069	9	11983	+1141	1331	+9.5	+7266	
2070	8	9133	-217	1142	-2.4	+7049	
2071	2	2307	-303	1154	-13.1	+6746	
2072	5	6749	+385	1350	+5.7	+7131	
2073	12	16960	-446	1413	-2.6	+6685	
2074	10	14890	-958	1489	-6.4	+5727	
2075	9	9105	-569	1012	-6.2	+5158	
2076	7	6868	+140	981	+2.0	+5298	
2077	9	7055	-259	784	-3.7	+5039	
2078	8	8519	-99	1065	-1.2	+4940	
2079	12	11140	+1204	928	+10.8	+6144	
2080	8	7772	+516	972	+6.6	+6660	

Continuation Table II

Rot.	n	E + W	E - W	$\frac{E + W}{n}$	$\frac{E - W}{E + W}$	$\Sigma(E - W)$	Rot.	n	E + W	E - W	$\frac{E + W}{n}$	$\frac{E - W}{E + W}$	$\Sigma(E - W)$
2081	6	6121	-49	1020	-0.8	+6611	2086	14	12736	+172	910	+1.3	+2739
2082	1	789	+87	789	+11.0	+6698	2087	11	10211	-2305	988	-22.6	+434
2083	4	3472	-612	868	-17.6	+6086	2088	14	12039	+377	860	+3.1	+811
2084	12	10083	-2501	840	-24.8	+3585	2089	13	12107	-911	931	-7.3	-100
2085	11	9292	-1018	845	-10.9	+2567							

Table II
Red line (6374A)

Alma Ata

Climax

Rot.	n	E + W	E - W	$\frac{E - W}{n}$	$\frac{E - W}{E + W}$	$\Sigma(E - W)$	Rot.	n	E + W	E - W	$\frac{E + W}{n}$	$\frac{E - W}{E + W}$	$\Sigma(E - W)$
2038	6	3331	-63	555	-1.9	-63	2009	3	2658	+116	886	+4.4	+5087
2039	7	3069	+171	438	+5.6	+108	2010	6	5404	-354	901	-6.6	+4733
2040	-	-	-	-	-	+108	2011	4	2454	-698	614	-28.4	+4035
2041	1	434	+22	434	+5.1	+130	2012	6	3932	-412	655	-10.5	+3623
2042	4	1530	-52	383	-3.4	+78	2013	11	8967	+93	815	+1.0	+3716
2043	-	-	-	-	-	+78	2014	4	3062	+482	766	+15.7	+4198
2044	-	-	-	-	-	+78	2015	9	8907	-3	990	0.0	+4195
2045	1	346	-2	346	-0.6	+76	2016	11	10097	+245	918	+2.4	+4440
2046	12	5656	+20	471	+0.4	+96	2017	18	20619	-921	1146	-4.5	+3519
2047	8	2807	+187	351	+6.7	+283	2018	16	18893	+29	1181	+0.2	+3848
2048	7	2094	-290	299	-13.8	-7	2019	20	20886	+424	1045	+2.0	+3972
2049	9	2765	-89	307	-3.2	-96	2020	16	21126	-2208	1320	-10.4	+1764
2050	2	883	+143	442	+16.2	+47	2021	12	14555	+507	1213	+3.5	+2271
2051	10	3909	+335	391	+8.6	+382	2022	15	16522	-874	1102	-5.3	+1397
2052	4	1003	-203	251	-20.2	+179	2023	11	16527	-307	1502	-1.9	+1090
2053	7	1572	+12	225	+0.8	+191	2024	4	5319	+475	1330	+8.9	+1565
2054	5	1200	+8	240	+0.7	+199	2025	-	-	-	-	+1565	
2055	5	1404	-242	281	-17.2	-43	2026	4	5136	+848	1284	+16.5	+2413
2056	1	144	-	144	-	-43	2027	4	5146	0	1286	0.0	+2413
2057	-	-	-	-	-	-43	2028	5	6314	-669	1268	-10.6	+1744
2058	-	-	-	-	-	-43	2029	6	7276	-382	1213	-5.2	+1362
2059	-	-	-	-	-	-43	2030	11	10807	+425	982	+3.9	+1787
2060	-	-	-	-	-	-43	2031	11	10232	+426	930	+4.2	+2213
2061	-	-	-	-	-	-43	2032	11	11451	+483	1041	+4.2	+2696
2062	-	-	-	-	-	-43	2033	14	14766	-716	1055	-4.8	+1980
2063	-	-	-	-	-	-43	2034	7	12366	+1416	1767	+11.5	+3396
2064	-	-	-	-	-	-43	2035	11	15570	+1302	1416	+8.4	+4698
2065	-	-	-	-	-	-43	2036	14	16668	+70	1191	+0.4	+4768
2066	1	193	+113	193	+58.5	+70	2037	7	8741	+601	1249	+6.8	+5369
2067	-	-	-	-	-	+70	2038	2	2389	-119	1194	-5.0	+5250
2068	-	-	-	-	-	+70	2039	5	4435	-13	887	-0.3	+5237
2069	-	-	-	-	-	+70	2040	9	13219	+1383	1469	+10.5	+6620
2070	-	-	-	-	-	+70	2041	2	2682	+214	1341	+8.0	+6834
2071	-	-	-	-	-	+70	2042	6	5678	-186	946	-3.3	+6648
2072	5	601	+355	120	+59.1	+425	2043	2	2093	-457	1046	-21.8	+6191
2073	3	427	-71	142	-16.6	+354	2044	3	3548	-858	1183	-24.2	+5333
2074	5	1320	+392	264	+29.7	+746	2045	8	10820	-626	1352	-5.8	+4707
2075	4	800	+572	200	+71.5	+1318	2046	11	14799	-741	1345	-5.0	+3966
2076	4	914	-332	229	-36.3	+986	2047	10	11434	-1299	1143	-11.4	+2667
2077	5	1010	+56	202	+5.5	+1042	2048	8	11032	-646	1379	-5.9	+2021
2078	5	1397	-21	279	-1.5	+1021	2049	7	9400	+512	1343	+5.4	+2533
2079	7	1035	-113	148	-10.9	+908	2050	4	4090	+438	1022	+10.7	+2971
2080	8	1795	+385	224	+21.4	+1293	2051	3	3422	+282	1141	+8.2	+3253
2081	3	588	+326	196	+55.4	+1619	2052	-	-	-	-	+3253	
2082	9	1424	+132	158	+9.3	+1751	2053	3	3451	-95	1150	-2.8	+3158
2083	4	1066	+122	267	+11.4	+1873	2054	1	865	+17	865	+2.0	+3175
2084	-	-	-	-	-	+1873	2055	-	-	-	-	+3175	
2085	13	2162	+308	166	+14.2	+2181	2056	8	7942	+418	993	+5.3	+3593
2086	15	10063	+1237	671	+12.3	+3418	2057	2	2525	-479	1262	-19.0	+3114
2087	10	2418	-528	242	-21.8	+2890	2058	3	3302	-164	1101	-5.0	+2950
2088	9	3398	-928	378	-27.3	+1962	2059	10	8917	-37	892	-0.4	+2913
2089	12	6451	-407	538	-6.3	+1555	2060	7	6971	-1857	996	-26.6	+1056

Continuation Table II

Rot.	n	E + W	E - W	$\frac{E + W}{n}$	$\frac{E - W}{E + W}$	$\Sigma(E - W)$	Rot.	n	E + W	E - W	$\frac{E + W}{n}$	$\frac{E - W}{E + W}$	$\Sigma(E - W)$
2061	11	11246	-427	1022	-4.2	+584	2066	5	715	+23	143	+3.2	-6486
2062	12	10109	-325	842	-3.2	+259	2067	8	1075	-99	134	-9.2	-6585
2063	9	9389	-69	1093	-0.7	+190	2068	5	893	-79	179	-8.8	-6664
2064	4	3288	-284	822	-8.6	-94	2069	6	1232	+278	205	+22.6	-6386
2065	1	791	+231	791	+29.2	+137	2070	12	2668	+424	222	+16.0	-5962
2066	-	-	-	-	-	+137	2071	16	5128	-188	320	-3.7	-6150
2067	3	2314	+10	771	+0.4	+147	2072	17	4012	+254	236	+6.3	-5896
2068	10	4833	-459	483	-9.5	-312	2073	13	3580	+204	275	+5.7	-5692
2069	9	5108	-130	568	-2.5	-442	2074	14	4479	+365	320	+8.1	-5327
2070	10	5435	+471	544	+8.7	+29	2075	14	4808	+650	343	+13.5	-4677
2071	8	8522	+548	1065	+6.4	+577	2076	10	3669	+501	367	+13.6	-4176
2072	11	9739	+489	885	+5.0	+1066	2077	10	3079	+579	308	+18.8	-3597
2073	12	13837	+2071	1153	+15.0	+3137	2078	11	2253	+493	205	+21.9	-3104
2074	8	9479	-1101	1185	-11.6	+2036	2079	10	2211	+271	221	+12.2	-2833
2075	3	3724	-340	1241	-9.1	+1696	2080	2	383	+225	191	+58.7	-2608
2076	9	8149	+781	905	+9.6	+2477	2081	11	1943	-187	177	-9.6	-2795
2077	7	5453	+641	779	+11.7	+3118	2082	6	829	+97	138	+11.7	-2698
2078	15	14057	+305	937	+2.2	+3423	2083	6	585	-47	98	-8.0	-2745
2079	6	5219	-169	870	-3.2	+3254	2084	5	1085	+187	217	+17.2	-2558
2080	4	2827	+31	707	+1.1	+3285	2085	11	1825	+421	166	+23.1	-2137
2081	1	744	+92	744	+12.4	+3377	2086	14	1395	+385	100	+27.6	-1762
2082	-	-	-	-	-	+3377	2087	15	3119	+9	208	+0.3	-1743
2083	3	1078	+202	359	+18.7	+3579	2088	12	4301	-95	358	-2.2	-1838
2084	10	4420	+176	442	+4.0	+3755	2089	6	1675	+33	279	+2.0	-1805
2085	3	1476	+240	492	+16.3	+3995	2090	8	1611	-63	201	-3.9	-1868
2086	7	3069	-349	438	-11.4	+3646							
2087	9	4976	-552	553	-11.1	+3094							
2088	14	10831	+2129	774	+19.6	+5223							
2089	7	3754	-184	536	-4.9	+5039							

Pic du Midi

Rot.	n	E + W	E - W	$\frac{E + W}{n}$	$\frac{E - W}{E + W}$	$\Sigma(E - W)$	Rot.	n	E + W	E - W	$\frac{E + W}{n}$	$\frac{E - W}{E + W}$	$\Sigma(E - W)$
2031	19	2847	-455	150	-16.0	-455	2010	4	2456	+410	640	+16.7	+12820
2032	18	4718	+374	262	+7.9	-81	2011	1	374	+100	374	+26.7	+12920
2033	15	9026	-1108	614	-12.3	-1189	2012	12	6483	+973	540	+15.0	+13893
2034	16	8592	-1034	537	-12.0	-2223	2013	3	2094	+176	698	+8.4	+14069
2035	16	8660	-178	541	-2.1	-2401	2014	1	556	+68	556	+12.2	+14137
2036	4	934	-404	234	-43.2	-2805	2015	7	3523	+525	503	+14.9	+14662
2037	5	1742	-364	348	-20.9	-3169	2016	5	2634	-38	527	-1.4	+14624
2038	8	2880	+156	360	+5.4	-3013	2017	13	7634	+42	587	+0.6	+14666
2039	5	1836	-78	367	-4.2	-3091	2018	14	9492	+518	678	+5.5	+15184
2040	7	2554	+398	365	+15.6	-2693	2019	4	4363	+427	1091	+9.8	+15611
2041	8	2720	-38	340	-1.4	-2731	2020	3	2799	+329	933	+11.8	+15940
2042	10	2306	-150	231	-6.5	-2881	2021	5	3103	+147	621	+4.7	+16087
2043	11	4541	+1369	413	+30.1	-1512	2022	6	4600	+604	767	+3.1	+16691
2044	11	4637	-437	422	-9.4	-1949	2023	1	731	+75	731	+10.3	+16776
2045	17	5905	-1061	347	-18.0	-3010	2024	5	3178	+576	636	+18.1	+17342
2046	14	5326	+16	380	+0.3	-2994	2025	2	1269	+161	634	+12.7	+17503
2047	18	6522	-356	362	-5.5	-3350	2026	4	3150	+696	787	+22.1	+18199
2048	16	4717	-469	295	-9.9	-3819	2027	2	1963	+193	981	+9.8	+18392
2049	12	3590	-1218	299	-33.9	-5037	2028	2	1220	-8	610	-0.7	+18384
2050	10	3901	-179	390	-4.6	-5216	2029	-	-	-	-	-	+18384
2051	7	3586	-82	512	-2.3	-5298	2030	1	375	-19	375	-5.1	+18365
2052	6	1173	-247	196	-21.1	-5545	2031	-	-	-	-	-	+18365
2053	12	2321	+195	193	+8.4	-5350	2032	4	3181	+253	795	+8.0	+18618
2054	12	4196	+86	350	+2.0	-5264	2033	-	-	-	-	-	+18618
2055	3	547	+25	182	+4.6	-5239	2034	5	4463	+339	893	+7.6	+18957
2056	6	1721	+307	304	+17.8	-4932	2035	-	-	-	-	-	+19137
2057	12	4866	+46	406	+0.9	-4886	2036	8	7302	+180	913	+2.5	+19137
2058	12	3944	+516	329	+13.1	-4370	2037	-	-	-	-	-	+19137
2059	16	7403	-1183	463	-16.0	-5553	2038	6	5387	+743	898	+13.8	+19880
2060	10	4732	+2	473	0.0	-5551	2039	1	881	+171	881	+19.4	+20051
2061	11	4738	-370	431	-7.8	-5921	2040	-	-	-	-	-	+20051
2062	4	2127	-21	532	-1.0	-5942	2041	5	2837	+495	567	+17.5	+20546
2063	6	3262	-66	544	-2.0	-6008	2042	1	514	+14	514	+2.7	+20560
2064	9	2950	-386	328	-13.1	-6394	2043	1	419	-41	419	-9.8	+20519
2065	6	2105	-115	351	-5.5	-6509	2044	4	2038	+204	510	+10.0	+20723
							2045	-	-	-	-	-	+20723
							2046	2	1591	+341	796	+21.4	+20382
							2047	2	-	-	-	-	+20382
							2048	3	1601	+179	534	+11.2	+20561

Continuation Table II

Rot.	n	E + W	E - W	$\frac{E + W}{n}$	$\frac{E - W}{E + W}$	$\Sigma(E - W)$	Rot.	n	E + W	E - W	$\frac{E + W}{n}$	$\frac{E - W}{F + W}$	$\Sigma(E - W)$
2049	—	—	—	—	—	+20561	2029	18	18410	+374	1023	+2.0	+4746
2050	—	—	—	—	—	+20561	2030	2	2152	-282	1076	-13.1	+4464
2051	1	424	-180	424	-42.5	+20381	2031	—	—	—	—	—	+4464
2052	1	201	-35	201	-17.4	+20346	2032	—	—	—	—	—	+4464
2053	—	—	—	—	—	+20346	2033	—	—	—	—	—	+4464
2054	—	—	—	—	—	+20346	2034	—	—	—	—	—	+4464
2055	—	—	—	—	—	+20346	2035	—	—	—	—	—	+4464
2056	9	9309	+667	1034	+7.2	+21013	2036	—	—	—	—	—	+4464
2057	5	14328	-1520	2866	-10.6	+19493	2037	9	8864	+662	985	+7.5	+5126
2058	5	10077	+9	2015	+0.0	+19502	2038	4	5713	-757	1428	-13.2	+4369
2059	4	9267	-619	2317	-6.7	+18883	2039	4	3696	+638	924	+17.3	+5007
2060	—	—	—	—	—	+18883	2040	9	13219	+1383	1469	+10.5	+6390
2061	4	1708	+190	427	+11.1	+19073	2041	8	11482	-212	1435	-1.8	+6178
2062	—	—	—	—	—	+19073	2042	5	6576	-242	1315	-3.7	+5936
2063	—	—	—	—	—	+19073	2043	8	13138	+1972	1642	+15.0	+7908
2064	2	301	-27	151	-9.0	+19046	2044	6	8544	-250	1424	-2.9	+7658
2065	1	626	+82	626	+13.1	+19128	2045	2	2691	-113	1346	-4.2	+7545
2066	—	—	—	—	—	+19128	2046	2	4355	+227	2178	+9.3	+7772
2067	—	—	—	—	—	+19128	2047	7	10899	-521	1557	-4.8	+7251
2068	1	3658	+6	3658	+0.2	+19134	2048	8	13158	+412	1645	+3.1	+7663
2069	1	4193	-33	4193	-0.8	+19101	2049	7	9279	-737	1326	-7.9	+6926
2070	—	—	—	—	—	+19101	2050	13	15902	+578	1223	+3.6	+7504
2071	3	9633	+317	3211	+3.3	+19418	2051	10	10639	+415	1064	+3.9	+7919
2072	1	2923	+637	2923	+21.8	+20055	2052	13	14414	+1382	1109	+9.6	+9291
2073	2	4226	+592	2113	+14.0	+20647	2053	5	5411	+793	1082	+14.7	+10084
2074	1	4828	-726	4828	-15.0	+19921	2054	7	7170	-336	1024	-4.7	+9748
2075	—	—	—	—	—	+19921	2055	6	5638	+18	940	+0.3	+9766
2076	—	—	—	—	—	+19921	2056	8	7687	-87	961	-1.1	+9679
2077	—	—	—	—	—	+19921	2057	3	2353	+105	784	+4.5	+9784
2078	—	—	—	—	—	+19921	2058	3	3391	-139	1130	-4.1	+9645
2079	—	—	—	—	—	+19921	2059	2	2238	-436	1119	-19.5	+9209
2080	16	6196	+1234	387	+19.9	+21155	2060	4	3005	+377	751	+12.6	+9586
2081	4	2301	+641	575	+27.8	+21796	2061	5	3323	-23	665	-0.7	+9563
2082	3	1220	+362	407	+29.7	+22158	2062	9	4468	+156	496	+3.5	+9719
2083	3	978	+58	326	+5.9	+22216	2063	4	1905	+93	476	+4.9	+9812
2084	7	3067	-13	438	-0.4	+22203	2064	3	1625	-55	542	-3.4	+9757
2085	6	3074	-192	512	-6.2	+22011	2065	4	2288	-130	572	-5.7	+9627
2086	—	—	—	—	—	+22011	2066	3	1698	+364	566	+21.4	+9991
2087	7	4258	+104	608	+2.4	+22115	2067	4	1982	+10	496	+0.5	+10001
2088	2	840	+126	420	+15.0	+22241	2068	—	—	—	—	—	+10001
2089	3	1330	-282	443	-21.2	+21959	2069	6	4737	+25	790	+0.5	+10026

Sacramento Peak

Rot.	n	E - W	E - W	$\frac{E + W}{n}$	$\frac{E - W}{E + W}$	$\Sigma(E - W)$
2010	14	5944	-286	425	-4.8	+5084
2011	5	2011	+279	402	+13.9	+5363
2012	14	6537	+11	467	+0.2	+5374
2013	13	9702	-408	746	-4.2	+4966
2014	15	13500	-580	900	-4.3	+4386
2015	9	7541	-617	838	-8.2	+3769
2016	4	2830	+176	708	+5.9	+3945
2017	5	3547	-61	709	-1.7	+3884
2018	11	8281	-53	753	-0.6	+3831
2019	14	14246	-598	1018	-4.2	+3233
2020	18	15602	-1032	867	-6.6	+2201
2021	21	20792	-214	990	-0.8	+1987
2022	17	17053	-961	1003	+5.6	+2948
2023	16	18249	-127	1141	-0.7	+2821
2024	7	5994	+250	856	+4.2	+3071
2025	11	11282	+146	1026	+1.3	+3217
2026	11	11353	+391	1032	+3.4	+3608
2027	14	14622	+6	1044	+0.0	+3614
2028	12	11744	+758	979	+6.4	+4372

asymmetry (maximum in absolute value). This opposite asymmetry for the given two stations is also shown in Fig. 1 of Gnevyshev's paper (1963).

c) Arosa, Wendelstein and Kanzelhöhe use one and the same observational method—visual estimates. The courses of the curves of the cumulative sums for Kanzelhöhe and Wendelstein are roughly equal, but opposite to that found at Arosa. If we exclude the year 1948 for Kanzelhöhe (high negative asymmetry due most likely to instrumental error), the asymmetry it shows is positive up to rotation No. 1971, that is until about 1953. The course of the curve for the Wendelstein station is similar: it moderately rises up to rotation No. 1979. After these rotations, however, the curve of the cumulative sums goes down for either station, that is, the western limb prevails. The course of the curve for Arosa is reversed: the prevailing asymmetry is negative until 1952, as also found by Bouška (1951), then the curve starts climbing indicating, on the whole, positive asymmetry from rotation 1965 upward. The years of reversal coincided with a period of low solar activity.

d) Climax and Sacramento Peak, whose observational methods are also equal, show the following course in the curves of the cumulative sums: Climax hardly had any asymmetry until 1957 the curve varied about equilibrium position. Nor did Sacramento Peak show a systematic asymmetry until 1956; in the following year, however, its asymmetry curve steeply declined. At this station, observations were discontinued over a few rotations in 1957. By the end of 1957, asymmetry at either station was positive. The preceding series of corona observations was interfered with at both stations in that year.

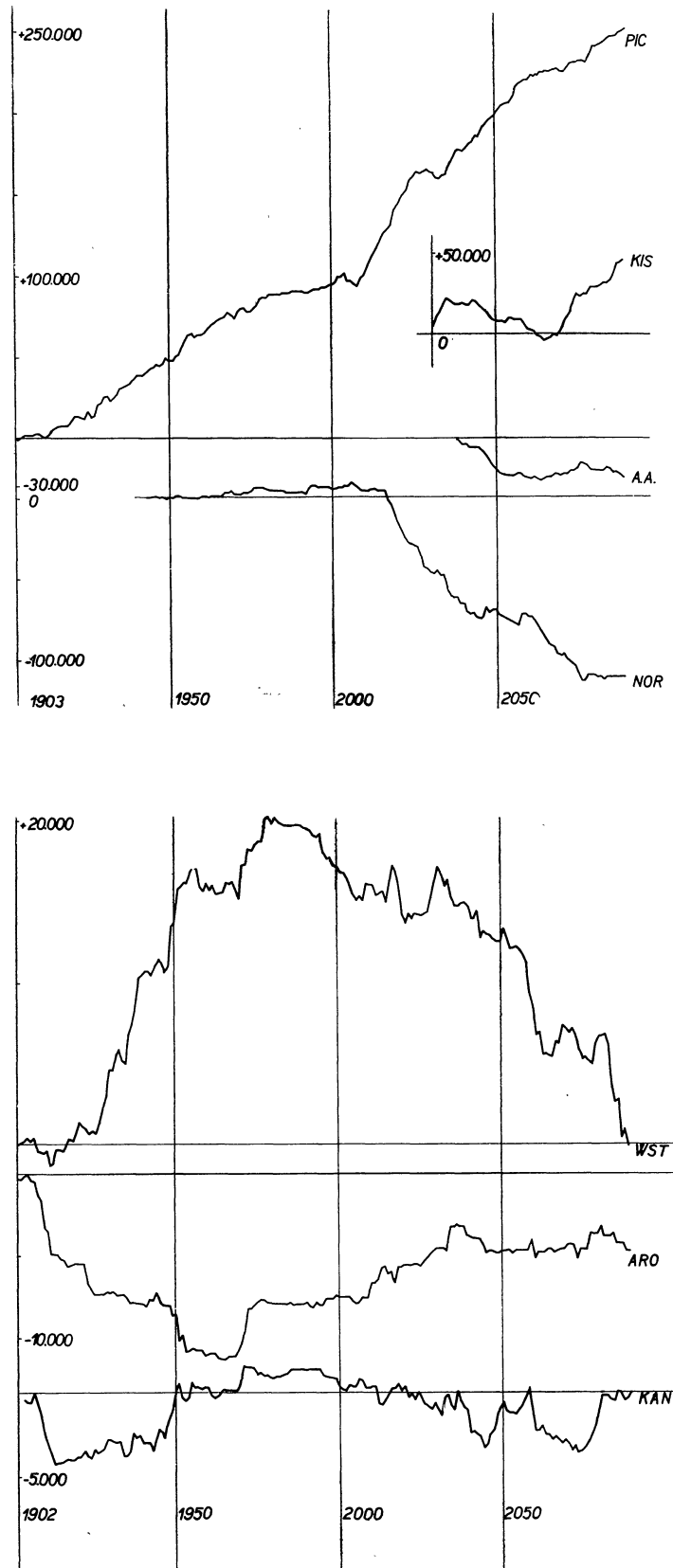


Figure 1. Curves of cumulative asymmetry sums $\Sigma(E - W)$ for the green line

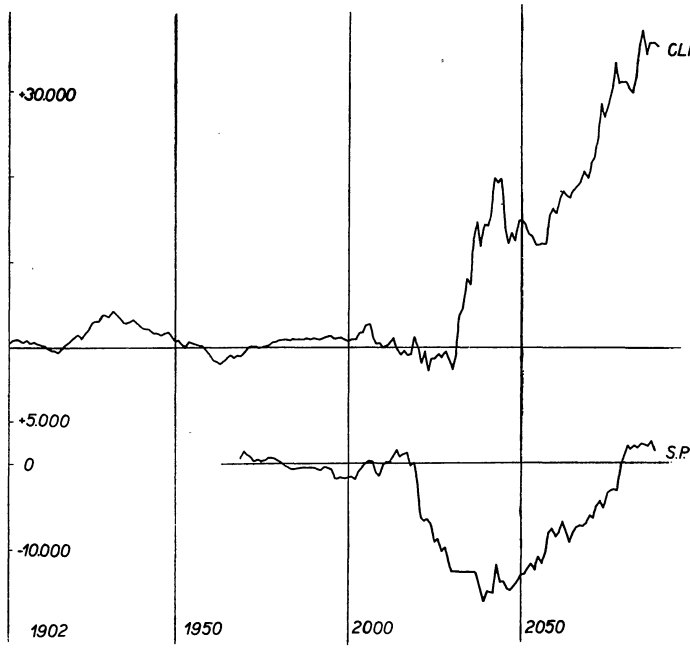


Figure 1c

e) The course in the curves of cumulative sums $\Sigma(E - W)$ for Kislovodsk and Alma Ata, the two last stations, is not equal either. If we disregard the initial rise in these sums at Kislovodsk from rotation No. 2038 to rotation No. 2065, that is until end 1959, then the initial asymmetry was negative for either station. From rotation No. 2066 on, the asymmetry for Kislovodsk was positive, while that for Alma Ata was still slightly negative, except for 1960, when it was positive.

None of the criteria—neither total asymmetry, nor the frequency of rotations with positive and negative asymmetry nor, eventually, the course in the curves of the cumulative sums—lead to an unambiguous conclusion on the asymmetry of the corona in the green line. The numerical values of total asymmetry with positive and negative signs show an approximately equal distribution, just as does the number of rotations with positive and negative asymmetry. The course of the curves of the cumulative sums reveals no systematic trend, each pair of stations showing both periods of equal and opposite variations. Positive and negative asymmetry alternate at all stations, except Pic du Midi, wherein no dependence may be detected.

Some periods with either high negative or high positive asymmetry evidently indicate

great local measuring errors. Such was—roughly—the year 1948 at the Kanzelhöhe station with high negative asymmetry, the year 1957 at Climax with high positive asymmetry, the preceding period in about 1956 at Sacramento Peak with negative asymmetry, and the year 1957 at Norikura with high negative asymmetry reaching as much as — 14.3 per cent. High asymmetry may be due to instrumental errors.

A relatively fairly smooth curve of cumulative sums with a systematic, almost uniform rise, that is a systematic positive asymmetry, was only found for Pic du Midi over the whole period in question. Hence we may conclude as follows:

Alternative 1. The measurements at Pic du Midi are correct, in other words, positive asymmetry has been proved.

Then, however, all the other stations must operate with a rather large systematic error, at least over certain periods, which even leads to negative asymmetry, that is to an asymmetry opposite to that found for Pic du Midi.

Alternative 2. Pic du Midi operates with an error resulting in a systematic prevalence of the

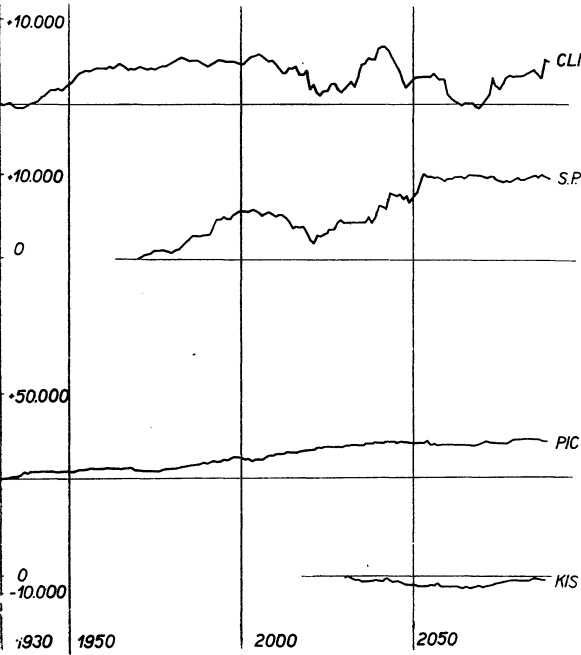


Figure 2. Curves of the cumulative asymmetry-sums $\Sigma(E - W)$ for the red line

Table III
Final total and relative asymmetry for period from 1948 until 1961
Green emission — 5303 Å

Station	Number of days	$\Sigma(E + W)$	$\Sigma(E - W)$	$\frac{\Sigma(E - W)}{\Sigma(E + W)} \%$
Alma Ata	291	742215	-21784	-2.93
Arosa	929	733389	-4782	-0.65
Climax	2476	3282125	+35358	+1.08
Kanzelhöhe	1369	1143768	-41	-0.004
Kislovodsk	675	2097046	+46108	+2.20
Pic du Midi	1759	4239583	+254179	+5.99
Norikura	750	1694678	-106231	-6.27
Sac. Peak	1255	1687341	+1435	+0.08
Wendelstein	1701	1679267	-100	-0.01
Red emission — 6374 Å				
Climax	1797	846951	+5039	+0.59
Kislovodsk	619	196178	-1805	-0.92
Pic du Midi	524	322812	+22803	+7.06
Sac. Peak	1209	697503	+9699	+1.39

Table IV
Distribution of relative asymmetry values $\frac{E - W}{E + W} \%$ over rotations Nos 1902 to 2089
Green emission

Station		$>\pm 50$	± 50	± 45	± 40	± 35	± 30	± 25	± 20	± 15	± 10	$\pm 5 \%$	
Alma Ata	E	—	—	—	—	—	1	1	1	3	1	4	
	W	—	—	—	—	—	—	2	1	3	9	11	
Arosa	E	1	—	1	1	—	1	3	4	2	9	21	
	W	—	—	—	—	1	2	3	1	5	11	27	
Climax	E	1	1	—	2	—	2	4	10	15	19	43	
	W	1	—	—	—	1	1	2	10	7	17	41	
Kanzelhöhe	E	1	—	—	1	—	1	4	2	8	15	40	
	W	2	1	—	—	—	—	2	3	6	12	47	
Kislovodsk	E	—	—	—	—	—	—	—	1	6	14	11	
	W	—	—	—	—	—	—	—	—	—	7	18	
Norikura	E	2	—	—	1	—	—	3	2	5	5	17	
	W	1	—	2	—	2	4	2	12	14	14	11	
Pic du Midi	E	1	1	1	2	2	4	4	15	27	46	34	
	W	—	—	—	2	—	—	—	2	3	7	23	
Sacramento Peak	E	—	—	1	1	—	1	—	2	8	13	30	
	W	—	—	—	—	—	—	1	—	8	12	24	
Wendelstein	E	—	—	—	1	3	3	3	5	4	28	38	
	W	2	1	—	1	1	—	5	8	7	21	47	
Red emission													
Climax	E	—	—	—	—	—	1	3	7	17	26	23	
	W	—	—	—	—	—	2	—	1	13	17	28	
Kislovodsk	E	—	—	—	—	1	1	3	5	5	6	7	
	W	—	—	1	—	1	—	2	3	3	10	10	
Pic du Midi	E	—	1	2	1	1	4	3	5	10	12	12	
	W	—	—	—	—	—	—	—	3	2	6	5	
Sacramento Peak	E	—	—	—	—	—	—	—	2	9	13	35	
	W	—	—	—	—	—	—	—	1	11	11	28	

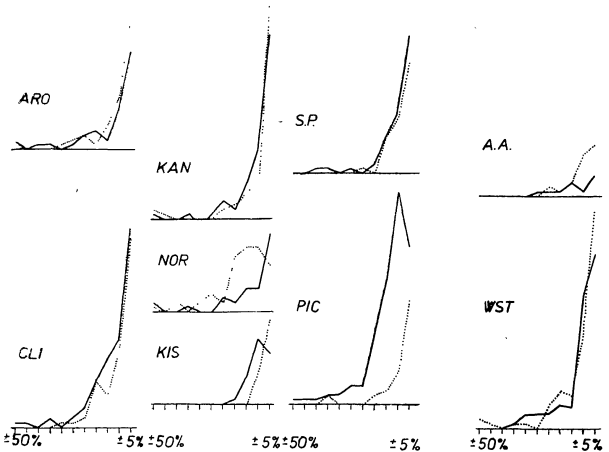


Figure 3. Distribution of relative asymmetry $\frac{(E - W)}{(E + W)} \%$

Table V

Number of rotations with positive and negative asymmetry
Green emission

Station	Number of rotations	0	0	0	0
		^	v	w	v
$E - W$					
Alma Ata	48	17	31	35.42	64.58
Arosa	134	65	69	48.51	51.49
Climax	185	102	83	55.14	44.86
Kanzelhöhe	175	87	88	49.71	50.29
Kislovodsk	59	32	27	54.24	45.76
Norikura	134	53	81	39.55	60.45
Pic du Midi	186	144	42	77.42	22.58
Sacr. Peak	113	61	52	53.98	46.02
Wendelstein	187	90	97	48.13	51.87
 Red emission					
Climax	153	87	66	56.86	43.14
Kislovodsk	59	30	29	50.85	49.15
Pic du Midi	116	82	34	70.69	29.31
Sacr. Peak	113	64	49	56.64	43.36

corona intensity in the East over that in the West. And since the remaining 8 stations fail to give an at least approximately equal measurement of the same phenomenon, we cannot determine, whether positive asymmetry does or does not exist. The measuring errors evidently are greater than the possible asymmetry.

With regard to the number of stations that show an asymmetry different from that of Pic du Midi, the second alternative must be considered incomparably more probable.

The presumed local error must be easiest to locate at Pic du Midi, as it is probable systematic in one direction, thus leading to an apparent

homogeneity of the observations. Hence we subjected these observations of Pic du Midi to certain tests.

4. Possible errors in measurements of the corona intensity

Systematic errors in the determination of the corona intensity may be due to: A. The observational method and the method of publishing the results, B. Atmospheric conditions and C. Instrumental errors.

A. Errors due to the observational method

The coronograph does not permit simultaneous measurements of the whole corona. The intensity of the spectral line of the corona is being estimated or photographed by 5° along the limb of the solar disk, which requires a certain time. The observational conditions, both atmospheric and instrumental (operation of the clock-drive i.e. the maintenance of the centre of the Sun in the coronograph axis, temperature) change during the observation. Another factor to consider is the adaptation and fatigue of the eye at visual estimates of the corona intensity. If the measurements are invariably started at a certain point on the solar limb, for instance in the North, and always continued in the same direction, such as over the East towards the South and back over the West to the North, then the possible error due to the change in any of the observational conditions depending on time affects differently individual quadrants. The final disturbing effect on a series of observations may remain relatively stable.

Should we succeed in proving an error that would depend on time and reduce, for instance, the intensity of the last against the first quadrants measured, then the fact that the measurements are systematically started at one point of the solar disc, for instance N, and that they are invariably conducted in one and the same direction, would have to be considered a relatively great error capable of resulting in asymmetry.

B. Errors due to varying atmospheric conditions

I. Effect of atmospheric conditions changing in the course of the day

Obviously, there is no sharp border line between conditions ideal and valueless for coronal observations. Moreover, it is psychologically natural if coronal observations are only started under "coronal conditions". However, these conditions need not necessarily stay unchanged until the

measurement is terminated, especially if it takes at least half an hour, if not more than an hour, before the round about the solar disc is completed. On the other hand, the observer does not start coronal observations under unfavourable conditions, and then there are no conditions that might improve. The number of cases, where the measurement terminates under poorer atmospheric conditions most likely exceeds that of the cases, where the atmospheric conditions may still improve.

According to the atmospheric conditions we distinguish four types of observations:

1. Observations under stable "coronal" atmospheric conditions. In this case, provided other errors are excluded, the asymmetry should show in its true value.

2. Observations stayed incomplete due to the fact that atmospheric conditions have deteriorated in their course. Such observations combined with the error in the observational method, as described above, give a great asymmetry in favour of the quadrants measured earlier than the others.

3. Observations completed under poorer atmospheric conditions which, in combination with the error in the observational method, also lead to a systematic proponderance of the first quadrant over the last one.

4. Observations under improving conditions are the least probable ones; they would lead to an asymmetry opposite to that in the preceding case.

Hence the observations systematically conducted from the northern point of the solar disc across the East lead to a great disadvantage of the western against the eastern limb.

Thus, if the first and second type of error combine, they may give a high asymmetry in favour of the East. The major part of our stations distinguish between cases, where the intensity of the corona could not be measured at some position angles and those, where the intensity of the corona was so low that it was immeasurable—in other words, where the intensity was 0 even under favourable conditions. However, Pic du Midi does not rank with them. No matter why the corona-intensity measurement is missing at any position angle, all the recordings show is a uniform—sign. This led us to investigate the striking cases of this station, where corona-intensity values are missing for one or more quadrants.

The number of quadrants with no readings on the intensity of the coronal line, that is the whole quadrant with the —sign for Pic du Midi, is given in Table VI.

Table VI

Quadrants	I.	II.	III.	IV.
Number of quadrants with no values for period from 1949 till 1961	31	60	113	138
For years 1956 till 1961	1	13	44	65

The table shows that the number of the quadrants with no measured values rises in the direction in which the observations of the corona about the solar disc are conducted at Pic du Midi. The reality of so high an asymmetry, as found for Pic du Midi, is virtually impossible. The other stations were subjected to the same examination. This was only done about maximum solar activity, with the intensity of the corona distributed, on the whole, equally around the disk. For Climax, Sacramento Peak, Norikura, Kanzelhöhe, Wendelstein, Alma Ata and Kislovodsk, cases, where the intensity of the corona was not measured owing to its very low value and cases, where it was not measured for other reasons, such as poorer observational conditions, were distinguished from each other by different signs. The results are listed in Table VII.

Table VII

Number of quadrants with no measured values for period from 1956 till 1959 (maximum solar activity)

Quadrant	I.		II.		III.		IV.	
Marking	—	x	—	x	—	x	—	x
<i>Station</i>								
Alma Ata	—	—	—	—	—	1	—	1
Arosa	—	—	—	—	—	—	—	—
Climax	2	6	1	10	1	37	—	38
Kanzelhöhe	—	15	4	15	—	16	—	16
Kislovodsk	—	1	—	6	—	14	—	13
Norikura	—	7	4	9	3	18	—	17
Pic du Midi	1	—	13	—	44	—	65	—
Sacr. Peak	—	2	—	1	—	5	—	1
Wendelstein	—	—	2	3	—	7	—	13

The table shows that the number of omitted measurements marked by x in the whole quadrants rises roughly from the 1st to the 4th quadrant. The number of the quadrants with no corona-intensity measurements, though the observational conditions were favourable (and hence marked 0, or, as the case may be, —) is so low, that it would be unreasonable to draw from this material any statistical conclusions on coronal asymmetry.

The unfavourable meteorological effect on the measurements at Pic du Midi is also borne out by

the fact that out of 65 cases with no measured values throughout the IVth quadrant between 1956 and 1959 (maximum solar activity) as much as 51 cases (78.5 %) showed values at position angles 5°, 10° and 15°. On the other hand, we did not record a single case, where the Ist quadrant throughout would have been without measurements, but values were determined at position angles 355°, 350° and 345°. The number of such cases on the solar South Pole is much lower; an empty IIIrd quadrant and values at three position angles east of the Pole were only found in three cases, while reversed cases did not occur at all. At the Climax station, out of 38 cases of empty IVth quadrants, only 9 cases — 23.6 % — showed values measured at the first three position angles of the Ist quadrant over the same period. Reversed cases did not occur at all. At the Climax station no such cases were recorded on the South Pole.

A difference between the asymmetry of the North and South Pole as large as recorded in this respect for Pic du Midi is not real; it is due to meteorological effects combined with the error in the observational method. It can be accounted for by the different time intervals between the measurements about the Poles: the measurements about the South Pole are made one after the other in close succession, while those about the North Pole (provided the measurements are started systematically at this point) are retarded by just as much as the duration of the complete measurement, so that the time interval between them is maximum.

It is safe to assume that no such days occur at the period about maximum solar activity, as would not include a measurable intensity value at any position angle throughout the quadrant—which for Pic du Midi is borne out by the Ist quadrant. Hence, days that may be considered incomplete measurements have been omitted from the statistics. Table VIII gives for all stations the number of days not included in the statistics, and separately the cases of not included days for the eastern and western quadrants. Considered were only the years about maximum solar activity, that is the period from 1956 till 1961.

The table giving the distribution of the days omitted due to a sudden and complete absence of further measurements, especially of empty quadrants, leads to the following two conclusions:

1. The large difference between the stations does not indicate that this asymmetry would be real.

Table VIII
Number of omitted days, where measurements were not completed

Station	Number of observational days	Number of days omitted					
				E		W	
		n	%	n	%	n	%
Alma Ata	122	2	1.6	—	—	2	100.0
Arosa	230	—	—	—	—	—	—
Climax	616	70	11.4	12	17.1	58	82.9
Kanzelhöhe	599	50	8.3	27	54.0	23	46.0
Kislovodsk	296	24	6.1	4	16.7	20	83.3
Norikura	392	43	14.5	21	48.8	22	51.2
Pic du Midi	552	62	11.2	3	4.8	59	95.2
Sacr. Peak	420	27	6.4	8	29.6	19	70.4
Wendelstein	512	24	4.7	5	20.8	19	79.2

2. The Arosa station most likely does not publish discontinued measurements, interrupted by atmospheric effects. The other stations publish them distinctly marked as such (except Pic du Midi), so that they can be safely eliminated. But we still have a third type of observations, where the measurement gets completed under already poorer atmospheric conditions. Such cases cannot be eliminated though they affect the measurements. At the Pic du Midi station, where the published cases are not distinguished by the x and — signs, positive asymmetry is relatively high and systematic.

The relative asymmetry in the distribution of the days eliminated as incomplete due to poorer atmospheric conditions is very high at Pic du Midi (up to 90.3 %) for the western quadrants, which naturally causes the asymmetry in the intensity of the corona to be positive.

Table IX
Relative asymmetry in days for which Pic du Midi has no values within at least one quadrant

Year	Pic du Midi	Climax	Kanzelhöhe	Norikura
1956	+69.7%	+4.3%	-1.8%	-15.2%
1957	+89.6	+4.6	+2.3	-4.9
1958	+85.8	+26.7	+3.7	-16.8
1959	+53.1	+1.4	-3.4	-5.4
1960	-15.9	+19.1	-4.7	+16.9
1961	+71.6	-0.2	-7.2	—

The asymmetry recorded at the Pic du Midi station on days that included at least one quadrant with no measured coronal-intensity value, as given in Table IX, is very high if compared with that of other three selected stations for the same days. This can be only explained by accumulation

of the error in the observational method and that due to atmospheric conditions. The rather high variation in the asymmetry found for the other stations is due to the low number of days.

II. Months with favourable and unfavourable observational conditions

Although the preceding consideration suffices to illustrate the unfavourable effect of atmospheric conditions on coronal measurements, we are not yet through with our argumentation.

The observational conditions on Mt Lomnický štít, where the first coronal measurements were made in 1964, are best during the early autumn months with their sizable anticyclones. The most unfavourable months, on the other hand, are November and February, and for day-time observations also the summer months, as they show a tendency towards diurnal orographic cloud-formation. If it were true for all stations that their atmospheric conditions change in the course of the year, this would have chiefly to show in the number of observational days. Table X lists the number of observational days at both Pic du Midi and Norikura in the individual months from 1956 till 1961.

asymmetry of the corona in detriment to the quadrants measured last.

Accordingly we only investigated the asymmetry for the two rotations that coincided with July and August and those two spring rotations

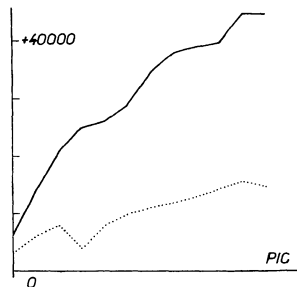


Figure 4. Cumulative asymmetry sums $\Sigma(E - W)$ a Pic du Midi for July and August (full line) and April, May (dotted line)

that mainly covered April. As to Norikura, we examined two rotations that covered the months with maximum observational days, and two summer months—June and July—where diurnal cloud-formation could be presumed. The numerical results are listed in Table XI.

Table X

Month	I.	II.	III.	IV.	V.	VI.	VII.	VIII.	IX.	X.	XI.	XII.
Pic du Midi	61	66	77	40	66	76	96	108	72	75	61	50
Norikura	23	23	37	50	33	33	35	40	36	50	63	37

The table shows that observational conditions on Pic du Midi were best in July and August, and poorest in April. Any tendency at this station towards diurnal cloud-formation in April and stabilization of weather conditions in the last summer months would certainly act on the

The results for Pic du Midi fully bore out the assumption: The asymmetry of rotations in months with unfavourable atmospheric conditions was much higher than of those in months with stabilized weather. Nothing justifies the assumption that this difference is real, since even the presumed

Table XI
Asymmetry in selected rotations

Station	n	Omitted quadrants	$\Sigma(E + W)$	$\Sigma(E - W)$	$\frac{\Sigma(E - W)}{n}$	$\frac{E - W}{E + W} \%$	Months
Pic du Midi	179	6 0.84 %	502687	+15185	+84.8	+3.0 %	July August
Norikura	94	8 2.1 %	351402	-33822	-359.8	-9.6 %	October November
Pic du Midi	120	30 6.25%	344745	+45323	+377.7	+13.1 %	March April
Norikura	52	18 8.65%	160834	-5568	-107.1	-3.5 %	June July

unfavourable effect of the Earth on the asymmetry (Kopecký, Mayer 1951; Kopecký, Mayer, Borovičková 1952) is lost in this case, the months under consideration not coinciding with the perihelium and aphelion of the Earth.

Norikura also substantiated our assumption in the sense that negative asymmetry in the summer months is suppressed by the effect of the atmospheric conditions which lead to positive asymmetry, provided the measurements are made from N over E, S and W back to N. This assumption is justified by the fact that 15 out of the 18 omitted quadrants were on the western limb.

III. Measurements in morning and afternoon hours

If we assume that the atmospheric conditions on Pic du Midi—just as on Mt Lomnický štít—are better in the morning than afternoon hours, this also should show by an increased asymmetry in favour of the eastern limb in observations made in the afternoon hours. Accordingly we investigated the asymmetry of the corona from measurements made in morning and afternoon hours.

The morning and afternoon observations for our analysis had to be made at Pic du Midi till 10 hours observing UT and from 12 hours UT on respectively (as shown by time mark), which practically agrees with the local time of that station.

The statistical result for Pic du Midi between 1956 and 1961 is as follows:

A ... number of observations in morning hours	... 316
B ... number of observations in afternoon hours	... 119

The number of the individual quadrants with no measured values is listed in Table XII.

Table XII

Case	Quadrants				Sum	%
	I.	II.	III.	IV.		
A	1	6	13	19	39	12.3
B	—	4	22	29	55	46.1

Almost all cases with no measurements in the IIIrd and IVth quadrant were most likely made at a period that did not coincide with minimum solar activity and stayed incomplete due to poor atmospheric conditions (see table IX).

The asymmetry in these selected days with morning and afternoon observations is as follows:

A ... cumulative sum of E — W asymmetry
82 277

B ... cumulative sum of E — W asymmetry
64 985

If we take into account the number of observational days, then the average asymmetry-increase per day is 260 units for case A and 546 units for case B. The average relative asymmetry for the morning measurements is 8.8 per cent, for the afternoon measurements as much as 19.8 per cent.

This great difference between the asymmetry of coronal intensity in the morning and afternoon hours cannot be considered real; it can only be explained as a consequence of atmospheric conditions, which deteriorate much more rapidly in the afternoon hours, while they are better and stabler in the morning hours.

IV. The E — W asymmetry on the northern and southern hemisphere

If it is correctly assumed that the Pic du Midi station operates with a systematic error to the detriment of the western half of the solar disc due to increasing cloud formation and deteriorating conditions in the course of the day, combined with the error in the observational method, then the asymmetry of the northern hemisphere must exceed that of the southern hemisphere (naturally of uncorrected values together with the days with incomplete measurements). The measurements of the southern quadrants closely succeed each other, so that the changing atmospheric conditions affect them almost equally. The northern quadrants, on the other hand, are frequently measured under atmospheric conditions largely changed. At the Pic du Midi station, the cumulative sum of E — W asymmetry increased to $\Sigma(NE - NW) = 110233$ on the northern and $\Sigma(SE - SW) = 99661$ on the southern hemisphere. This is another result to show that the assumption of an unfavourable effect of the deteriorating atmospheric conditions on the measurements of the coronal intensity in favour of positive asymmetry is correct.

C. Instrumental errors

On the basis of the foregoing papers by other authors (Waldmeier 1955, Link and Lincová 1956) we shall assume that incorrectly centred optical elements, diaphragms and artificial moons as well as inaccurate guiding of the

Sun's centre in the coronagraph axis may result in instrumental errors and these, in turn, in systematically incorrect measurements of the intensity of the coronal line around the perimeter of the solar disc.

We analysed the distribution of the maxima and minima of the measured intensities in whole quadrants as well as their mutual positions, and arrived at interesting results.

It need not be assumed that a certain mutual position of the quadrants with maximum and minimum coronal-intensity values, as recorded at one station, would not be duplicated at other stations; less reasonable is the case where—for a certain station—the change in the quadrant of the minimum is associated with the change in the quadrant

Table XIII
Distribution of maximum corona-intensity values in individual quadrants

Station	Number of rotations	Quadrant				
		I.	II.	III.	IV.	
Alma Ata	40	n %	21 52.50	2 5.00	0 0	17 42.50
Arosa	56	n %	33 58.93	8 14.29	6 10.71	9 16.07
Climax	79	n %	33 41.77	13 16.46	8 10.13	25 31.64
Kanzelhöhe	80	n %	19 23.75	14 17.50	13 16.25	34 42.50
Kislovodsk	55	n %	40 72.72	2 3.64	5 9.09	8 14.55
Norikura	74	n %	20 27.03	7 9.46	12 16.22	35 47.29
Pic du Midi	79	n %	48 60.76	17 21.52	1 1.27	13 16.45
Sacramento Peak	72	n %	40 55.56	4 5.55	10 13.89	18 25.00
Wendelstein	80	n %	23 28.75	10 12.50	5 6.25	42 52.50

of the maximum, especially if the other station shows a tendency towards the reversed phenomenon. Thus we cannot consider real, for instance, the case, where, if the maximum passes from the first quadrant into the second, the minimum systematically passes from the third quadrant into the fourth.

Table XIV
Distribution of minimum corona-intensity values in individual quadrants

Station	Number of rotations	Quadrant				
		I.	II.	III.	IV.	
Alma Ata	40	n %	0 0	23 57.50	17 42.50	0 0
Arosa	56	n %	5 8.93	25 44.64	11 19.64	15 26.79
Climax	79	n %	7 8.86	16 20.25	44 55.70	12 15.19
Kanzelhöhe	80	n %	13 16.25	15 18.75	38 47.50	14 17.50
Kislovodsk	55	n %	3 5.45	27 49.09	22 40.00	3 5.46
Norikura	74	n %	15 20.27	34 45.95	20 27.03	5 6.75
Pic du Midi	79	n %	3 3.80	5 6.33	54 68.35	17 21.52
Sacramento Peak	72	n %	12 16.67	24 33.33	31 43.06	5 6.94
Wendelstein	80	n %	10 12.50	21 26.25	41 51.25	8 10.00

Tables XIII to XV give the distribution of maximum and minimum intensities of the corona in the individual quadrants. Table XVI lists the number of cases A, where the maxima and minima lie in neighbouring quadrants, and the number of cases B, where they lie in opposite quadrants.

The analysis of this aspect, as made for a few stations, is as follows:

1. At Pic du Midi, the number of cases B was

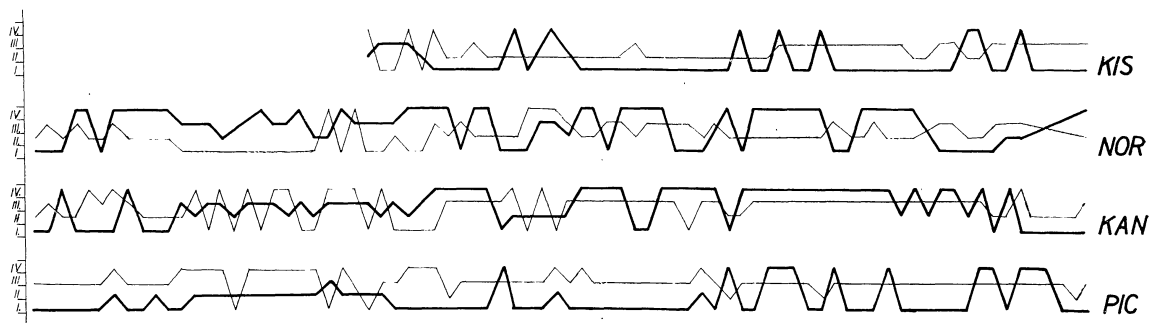


Figure 5. Course of quadrants with maximum measured corona-intensity value (thick line) and minimum value (thin line)

Table XV
Number of minimum intensity values in individual quadrants as against maximum values

Station	Number of maxima	Number of minima in individual quadrants							
		I.		II.		III.		IV.	
Quadrant	n	%	n	%	n	%	n	%	
Alma Ata									
I.	21	—	—	13	61.9	8	38.1	0	0
II.	2	0	0	—	—	2	100.0	0	0
III.	0	0	0	0	0	—	—	0	0
IV.	17	0	0	10	58.8	7	41.2	—	—
Arosa									
I.	32	—	—	19	57.6	9	27.3	5	15.1
II.	8	2	25.0	—	—	0	0	6	75.0
III.	6	1	16.7	1	16.6	—	—	4	66.7
IV.	9	2	22.2	5	55.6	2	22.2	—	—
Climax									
I.	33	—	—	10	30.3	22	66.7	1	3.0
II.	13	5	38.5	—	—	3	23.1	5	38.4
III.	8	2	25.0	0	0	—	—	6	75.0
IV.	25	0	0	6	24.0	19	76.0	—	—
Kanzelhöhe									
I.	19	—	—	10	52.6	6	31.6	3	15.8
II.	14	5	35.7	—	—	4	28.6	5	35.7
III.	13	6	46.2	1	7.7	—	—	6	46.1
IV.	34	2	5.9	4	11.8	28	82.3	—	—
Kislovodsk									
I.	40	—	—	20	50.0	19	47.5	1	2.5
II.	2	1	50.0	—	—	0	0	1	50.0
III.	5	2	40.0	2	40.0	—	—	1	20.0
IV.	8	0	0	5	62.5	3	37.5	—	—
Norikura									
I.	20	—	—	10	50.0	9	45.0	1	5.0
II.	7	2	28.6	—	—	4	57.1	1	14.3
III.	12	8	66.7	1	8.3	—	—	3	25.0
IV.	35	5	14.3	20	57.1	10	28.6	—	—
Pic du Midi									
I.	48	—	—	3	6.3	40	83.3	5	10.4
II.	17	2	11.8	—	—	3	17.6	12	70.6
III.	1	1	100.0	0	0	—	—	0	0
IV.	13	0	0	2	15.4	11	84.6	—	—
Sacramento Peak									
I.	40	—	—	14	35.0	24	60.0	2	5.0
II.	4	2	50.0	—	—	1	25.0	1	25.0
III.	10	8	80.0	0	0	—	—	2	20.0
IV.	18	2	11.1	10	55.6	6	33.3	—	—
Wendelstein									
I.	23	—	—	6	26.1	15	65.2	2	8.7
II.	10	3	30.0	—	—	1	10.0	6	60.0
III.	5	5	100.0	0	0	—	—	0	0
IV.	42	2	4.8	15	35.7	25	59.5	—	—

maximum, as much as 78.8 %. The maxima mostly occurred in the first and IIInd quadrant.

2. At Norikura, the station with the next highest number of cases B and asymmetry opposite to that at Pic du Midi, the greater part of the maxima lay in quadrants opposite to those at Pic du Midi, that is in the western quadrants. It is safe to say that, as to the distribution of maxima and minima, Pic du Midi and Norikura

Table XVI
Position of minimum as against maximum values in quadrants

Station	Number of rotations	A		B		Asymmetry %
		n	%	n	%	
Alma Ata	40	22	55.00	18	45.00	-2.93
Arosa	56	35	62.50	21	37.50	-0.65
Climax	79	44	55.70	35	44.30	+1.08
Kanzelhöhe	80	59	73.75	21	26.25	-0.004
Kislovodsk	55	28	50.91	27	49.09	+2.20
Norikura	74	33	44.59	41	55.41	-6.27
Pic du Midi	79	24	21.25	55	78.75	+5.99
Sac. Peak	72	43	59.72	29	40.28	+0.08
Wendelstein	80	39	48.75	41	51.25	-0.01

are almost mirror images. At the period with the maximum in the IIInd and minimum in the IVth quadrant at Pic du Midi, the minimum at Norikura lay chiefly (in as much as 85 % of all cases) in the Ist and the maxima (up to 78 %) in the IIIrd and IVth quadrant.

3. The maximum for Kanzelhöhe mostly (up to 87 %) occurred in the IVth quadrant over the period from rotation No. 2051 through to rotation No. 2074, that is over about 2 years, while that for Pic du Midi lay (in as much as 71 % of all cases) in the Ist quadrant over the same period.

4. At the Kislovodsk station the maximum occurred chiefly in the Ist quadrant. For the period from rotation No. 2041 to rotation No. 2065, that is roughly over two years, the minimum lays (up to 92 %) in the IIInd quadrant—in the following period (up to 83 %) in the IIIrd quadrant. At a certain period the maxima and minima of Kaznelhöhe and Kislovodsk were almost distributed mirror-image like.

Such cases cannot be considered real and, as they are entirely local even though prolonged, and as they exhibit certain changes, they can be only explained as a consequence of an instrumental error. Such instrumental errors, naturally individual for each station, may lead to completely reversed E—W asymmetries. Changes in the position and distribution of the maxima and minima at a given station may coincide with certain interferences with the instrument.

The effect of this error on E—W asymmetry comes best to the fore if we compare, for instance, the conditions at Pic du Midi and at the Kislovodsk station. At Pic du Midi, the maximum, as a rule, only moved from the Ist in the IIInd quadrant and vice versa, and the minimum only varied between the IIIrd and IVth quadrant, that is, the maximum stayed on the eastern and the minimum on the western limb, and the asymmetry did not

change, it was invariably positive. At the Kislovodsk station, negative asymmetry changed into positive as the position of the minimum in rotation 2066 changed with regard to the maximum by passing from the IIInd into the IIIrd quadrant.

Conclusion: It has been proved (in our opinion) that the asymmetry as determined at some stations is also influenced by certain errors in centring the optical elements of the coronograph. This conclusion is corroborated by the following facts:

1. The high percentage of opposite quadrants with maximum and minimum measured-intensity sums precisely at stations with highest asymmetry.
2. The dependence of the passage of the minimum on the passage of the maximum from one quadrant into the other is not real. This phenomenon is especially striking at Pic du Midi.

The North-South asymmetry

It is well known that the variable phenomena on the Sun are not symmetrically distributed with regard to the equator: the intensity of the activity is higher now on the northern, now on the southern hemisphere. Maximum and minimum solar activity do not coincide on both hemispheres (Waldmeier 1955, Brunner-Höger 1939, Brunner-Höger and Liepert 1941). The 19th cycle of solar activity coincided with a period, where the northern hemisphere prevailed.

Our investigation of the coronal N—S asymmetry was mainly aimed at determining how it shows at the individual stations and how the curves of cumulative sums $\Sigma(N - S)$ agree with each other. For the green line it was investigated from uncorrected values, that is from measurements as given in the QBSA. The sums of the measured corona-intensity values for the northern and southern hemisphere, together with the cumulative sum of the differences, are listed in Table XVII. The respective graph shows at first glance that the course of the N—S asymmetry

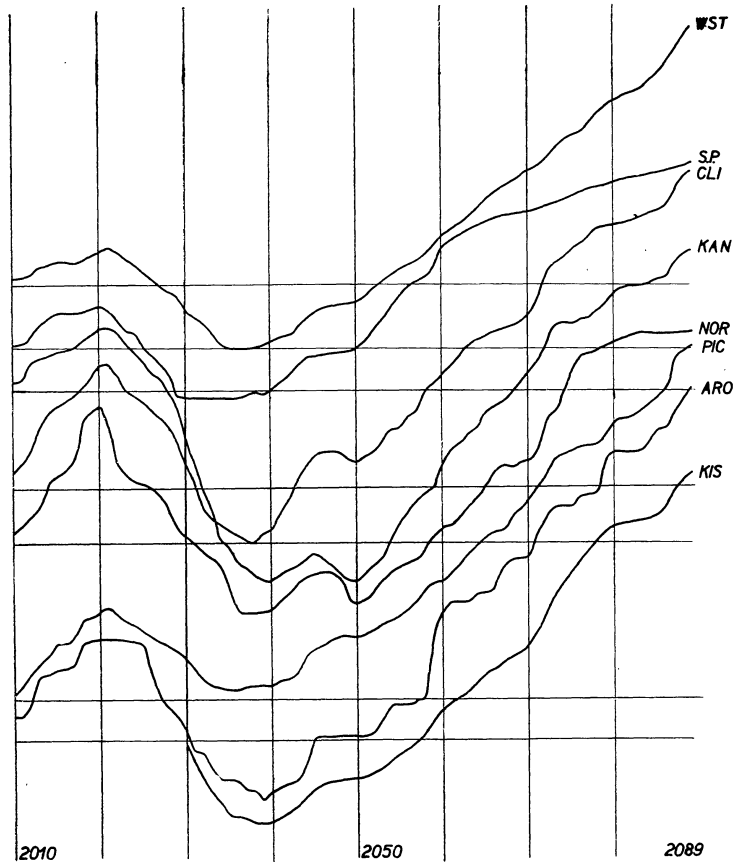


Figure 6. Curves of cumulative asymmetry-sums $\Sigma(N - S)$ for all stations

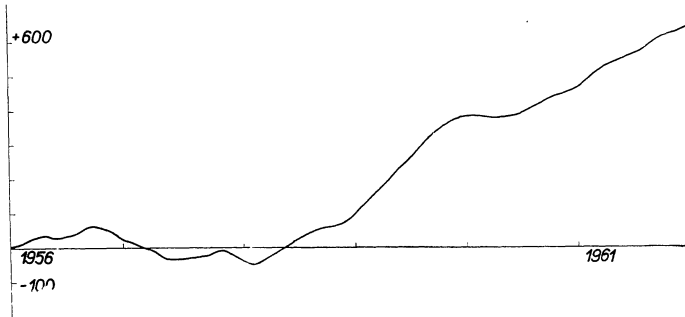


Figure 7. Cumulative asymmetry of the number of spot groups

curves for the period from 1956 till 1961 in question differed largely from that of the curves of the E—W asymmetry, expressed by cumulative sums. The curves of the N—S asymmetry were very much like the asymmetry variations that fell in the same period, some stations even agreed in minor fluctuations, and it is worth noting that it were precisely Pic du Midi and Norikura that did so. Just as in the distribution of sunspot groups (Publikation der Eidgenössischen Sternwarte, Zürich, 1956—1961) between the northern and

Table XVII
N — S asymmetry

Arosa

Rot.	N	S	N — S	$\Sigma(N - S)$	Rot.	N	S	N — S	$\Sigma(N - S)$
2010	3266	1824	+ 1442	+ 1442	2079	—	—	—	+ 14275
2011	—	—	—	+ 1442	2080	7960	5811	+ 2149	+ 16424
2012	2266	1586	+ 680	+ 2122	2081	2966	2644	+ 322	+ 16746
2013	4667	3081	+ 1586	+ 3708	2082	—	—	—	+ 16746
2014	500	374	+ 126	+ 3834	2083	—	—	—	+ 16746
2015	1424	1131	+ 293	+ 4127	2084	2269	1819	+ 450	+ 17196
2016	432	346	+ 86	+ 4213	2085	2575	1789	+ 786	+ 17982
2017	5844	5736	+ 108	+ 4321	2086	—	—	—	+ 17982
2018	10040	8660	+ 1380	+ 5701	2087	1432	671	+ 761	+ 18743
2019	6943	6786	+ 157	+ 5858	2088	3536	1825	+ 1711	+ 20454
2020	1309	1243	+ 66	+ 5924	2089	—	—	—	+ 20454
2021	—	—	—	+ 5924					
2022	—	—	—	+ 5924					
2023	1447	1576	- 129	+ 5795					
2024	—	—	—	+ 5795					
2025	496	633	- 137	+ 5658					
2026	8270	10168	- 1898	+ 3760					
2027	5227	6492	- 1265	+ 2495					
2028	723	1273	- 550	+ 1945					
2029	1513	2089	- 576	+ 1369					
2030	1535	2284	- 749	+ 620					
2031	2641	3984	- 1343	- 723					
2032	—	—	—	- 723					
2033	1610	2450	- 840	- 1563					
2034	4787	5569	- 782	- 2345					
2035	—	—	—	- 2345					
2036	1336	1439	- 103	- 2448					
2037	4857	5327	- 470	- 2918					
2038	—	—	—	- 2918					
2039	2621	3158	- 537	- 3455					
2040	6284	5963	+ 321	- 3134					
2041	1476	1188	+ 288	- 2846					
2042	1128	941	+ 187	- 2659					
2043	675	461	+ 214	- 2445					
2044	5473	4552	+ 921	- 1524					
2045	7998	6299	+ 1699	+ 175					
2046	1398	1402	- 4	+ 171					
2047	—	—	—	+ 171					
2048	552	544	+ 8	+ 179					
2049	—	—	—	+ 179					
2050	1492	1448	+ 44	+ 223					
2051	—	—	—	+ 223					
2052	2101	1957	+ 144	+ 367					
2053	5776	4995	+ 781	+ 1148					
2054	5496	4613	+ 883	+ 2031					
2055	—	—	—	+ 2031					
2056	481	490	- 9	+ 2022					
2057	2164	1906	+ 258	+ 2280					
2058	—	—	—	+ 2280					
2059	11113	7161	+ 3952	+ 6232					
2060	5013	4077	+ 936	+ 7168					
2061	2833	1968	+ 865	+ 8033					
2062	—	—	—	+ 8033					
2063	—	—	—	+ 8033					
2064	1904	1384	+ 520	+ 8553					
2065	—	—	—	+ 8553					
2066	919	748	+ 171	+ 8724					
2067	6498	5059	+ 1439	+ 10163					
2068	1008	781	+ 227	+ 10390					
2069	—	—	—	+ 10390					
2070	793	681	+ 112	+ 10502					
2071	—	—	—	+ 10502					
2072	3900	2379	+ 1521	+ 12023					
2073	2532	1585	+ 947	+ 12970					
2074	3233	2705	+ 528	+ 13498					
2075	—	—	—	+ 13498					
2076	—	—	—	+ 13498					
2077	2517	1837	+ 680	+ 14178					
2078	567	470	+ 97	+ 14275					
Climax									
2010	17393	9574	+ 7819	+ 7819					
2011	10482	4582	+ 5900	+ 13719					
2012	15349	9415	+ 5934	+ 19653					
2013	26993	12824	+ 14169	+ 33822					
2014	21665	12011	+ 9654	+ 43476					
2015	20862	17010	+ 3852	+ 47328					
2016	25566	24324	+ 1242	+ 48570					
2017	42044	38957	+ 3087	+ 51657					
2018	40577	33278	+ 7299	+ 58956					
2019	45688	41627	+ 4061	+ 63017					
2020	46356	38231	+ 8125	+ 71142					
2021	30160	29076	+ 1084	+ 72226					
2022	31843	37110	- 5267	+ 66959					
2023	31153	40934	- 9781	+ 57178					
2024	7666	10422	- 2756	+ 54422					
2025	3569	7206	- 3637	+ 50785					
2026	10380	14751	- 4371	+ 46414					
2027	10513	14444	- 3931	+ 42483					
2028	17395	22113	- 4718	+ 37765					
2029	25825	36945	- 11120	+ 26645					
2030	31231	43952	- 12721	+ 13924					
2031	27368	38850	- 11482	+ 2442					
2032	32475	45674	- 13199	- 10757					
2033	34567	42360	- 7793	- 18550					
2034	30682	33451	- 2769	- 21319					
2035	42569	45321	- 2752	- 24071					
2036	36421	39211	- 2790	- 26861					
2037	32590	35346	- 2756	- 29617					
2038	7795	10234	- 2439	- 32056					
2039	17222	12541	+ 4681	- 27375					
2040	10159	7551	+ 2608	- 24707					
2041	23776	16014	+ 7762	- 17005					
2042	27605	20043	+ 7562	- 9443					
2043	25195	15017	+ 10178	+ 735					
2044	28613	19839	+ 8774	+ 9509					
2045	48961	40233	+ 8728	+ 18237					
2046	39777	38373	+ 1404	+ 19641					
2047	36496	36215	+ 281	+ 19922					
2048	23842	23427	+ 415	+ 20337					
2049	23457	28342	- 4885	+ 15452					
2050	13601	14201	- 600	+ 14852					
2051	11735	9209	+ 2526	+ 17378					
2052	5023	2900	+ 2123	+ 19501					
2053	14188	7320	+ 6868	+ 26369					
2054	15860	9709	+ 6151	+ 32520					
2055	2055	—	—	+ 32520					
2056	23770	16599	+ 7171	+ 39691					
2057	10470	7364	+ 3106	+ 42797					
2058	26482	21013	+ 5469	+ 48266					
2059	43706	30653	+ 13053	+ 61319					
2060	9022	6695	+ 2327	+ 63646					
2061	25344	19920	+ 5424	+ 69070					
2062	23190	16078	+ 7112	+ 76182					
2063	25331	18713	+ 6618	+ 82800					

Continuation Table XVII

Rot.	N	S	N — S	$\Sigma(N - S)$	Rot.	N	S	N — S	$\Sigma(N - S)$
2064	8791	6137	+2654	+85454	2050	2763	2862	-99	-22170
2065	1631	1204	+427	+85881	2051	8482	7495	+987	-21183
2066	2808	1115	+1693	+87574	2052	13340	12621	+719	-20464
2067	12788	10070	+2718	+90292	2053	4334	3365	+989	-19495
2068	13920	12093	+1827	+92119	2054	6887	4722	+2165	-17330
2069	11321	9103	+2218	+94337	2055	5816	4126	+1690	-15640
2070	23414	17559	+5855	+100192	2056	3614	2234	+1380	-14260
2071	22623	16089	+6534	+106726	2057	6577	5131	+1446	-12814
2072	31244	17025	+14219	+120945	2058	5435	4719	+716	-12098
2073	27307	18556	+8751	+129696	2059	4322	3579	+743	-11355
2074	15663	12907	+2756	+132452	2060	9327	6762	+2565	-8790
2075	13250	9967	+3283	+135735	2061	9550	7821	+1729	-7061
2076	16849	11638	+5211	+140946	2062	3229	2601	+628	-6433
2077	12842	8583	+4259	+145205	2063	3224	1892	+1332	-5101
2078	17957	12263	+5694	+150899	2064	2981	2427	+554	-4547
2079	6586	5018	+1568	+152467	2065	4427	2675	+1752	-2795
2080	2724	2008	+716	+153183	2066	2841	1973	+868	-1927
2081	4130	3021	+1109	+154292	2067	1758	1363	+395	-1532
2082	3238	2788	+450	+154742	2068	2865	1902	+963	-569
2083	5310	4301	+1009	+155751	2069	3225	1904	+1321	+752
2084	12815	9254	+3561	+159312	2070	4287	3024	+1263	+2015
2085	5557	3824	+1733	+161045	2071	5793	4520	+1273	+3288
2086	10623	6983	+3640	+164685	2072	4884	3155	+1729	+5017
2087	16043	7809	+8234	+172919	2073	7339	4853	+2486	+7503
2088	16776	8693	+8083	+181002	2074	1657	1413	+244	+7747
2089	11134	6343	+4791	+185793	2075	946	995	-49	+7698
Kanzelhöhe									
2010	2534	1615	+919	+919	2076	4267	3691	+576	+8274
2011	1210	843	+367	+1286	2077	848	758	+90	+8364
2012	5303	3237	+2066	+3352	2078	4592	3755	+837	+9201
2013	703	188	+515	+3867	2079	5949	4742	+1207	+10408
2014	826	717	+109	+3976	2080	4386	3290	+1096	+11504
2015	1899	1207	+692	+4668	2081	1808	1349	+459	+11963
2016	804	805	-1	+4667	2082	389	212	+177	+12140
2017	3904	3529	+375	+5042	2083	706	652	+54	+12194
2018	5471	4620	+851	+5893	2084	828	626	+202	+12396
2019	5956	5342	+614	+6507	2085	3252	2541	+711	+13107
2020	7655	6836	+819	+7326	2086	3270	3055	+215	+13322
2021	7674	7648	+26	+7352	2087	6546	4769	+1777	+15099
2022	1879	2212	-333	+7019	2088	1664	827	+837	+15936
2023	4573	6019	-1446	+5573	2089	1119	674	+445	+16381
2024	5640	6579	-939	+4634	Kislovodsk				
2025	2755	3829	-1074	+3560	2030	9835	14071	-4236	-4236
2026	4232	5682	-1450	+2110	2031	25090	36145	-11055	-15291
2027	2218	2648	-430	+1680	2032	28294	37185	-8891	-24182
2028	4557	6331	-1774	-94	2033	28432	36432	-8000	-32182
2029	4143	6195	-2052	-2146	2034	35327	40794	-5467	-37649
2030	8215	11568	-3353	-5499	2035	29339	37035	-7696	-45345
2031	5109	7911	-2802	-8301	2036	8616	9601	-985	-46330
2032	4774	7959	-3185	-11486	2037	12281	13198	-917	-47247
2033	3853	5884	-2031	-13517	2038	11188	12750	-1562	-48809
2034	10420	14051	-3631	-17148	2039	8210	9189	-979	-49788
2035	5306	6231	-925	-18073	2040	9166	8615	+551	-49237
2036	7373	9027	-1654	-19727	2041	14894	12348	+2546	-46691
2037	6512	7424	-912	-20639	2042	20248	18001	+2247	-44444
2038	4894	5587	-693	-21332	2043	22117	18088	+4029	-40415
2039	2591	3229	-638	-21970	2044	23529	18705	+4824	-35591
2040	5347	5526	-179	-22149	2045	30400	26491	+3909	-31682
2041	6460	5731	+729	-21420	2046	24003	20206	+3797	-27885
2042	5481	4972	+509	-20911	2047	31153	29259	+1894	-25991
2043	4472	4118	+354	-20557	2048	27658	27180	+478	-25513
2044	10856	9931	+925	-19632	2049	18438	16492	+1946	-23567
2045	14375	13616	+759	-18873	2050	17914	18449	-535	-24102
2046	9493	10175	-682	-19555	2051	12018	10600	+1418	-22684
2047	5769	6363	-594	-20149	2052	11281	9301	+1980	-20704
2048	7739	8762	-1023	-21172	2053	19346	17027	+2319	-18385
2049	7425	8324	-899	-22071	2054	30042	23631	+6411	-11974
					2055	6542	4414	+2128	-9846

Continuation Table XVII

Rot.	N	S	N - S	$\Sigma(N - S)$	Rot.	N	S	N - S	$\Sigma(N - S)$
2056	19715	17318	+2397	-7449	2043	15127	12127	+3000	-15030
2057	22430	16756	+5674	-1775	2044	4952	2677	+2275	-12755
2058	21796	18516	+3280	+1505	2045	1430	1319	+111	-12644
2059	42134	32203	+9931	+11436	2046	10171	8700	+1471	-11173
2060	20997	16674	+4323	+15759	2047	11623	12114	-491	-11664
2061	23569	19217	+4352	+20111	2048	11089	13576	-2487	-14151
2062	11782	7583	+4199	+24310	2049	19587	25739	-6152	-20303
2063	12185	10372	+1813	+26123	2050	5612	5668	-56	-20359
2064	17559	11778	+5781	+31904	2051	4022	3274	+748	-19611
2065	17520	12280	+5240	+37144	2052	5090	2257	+2833	-16778
2066	9566	7663	+1903	+39047	2053	9323	6187	+3136	-13642
2067	18777	14353	+4424	+43471	2054	6559	4462	+2097	-11545
2068	9547	7139	+2408	+45879	2055	4132	2277	+1855	-9690
2069	13604	9992	+3612	+49491	2056	8473	7078	+1395	-8295
2070	24422	18749	+5673	+55164	2057	7504	6509	+995	-7300
2071	27598	21337	+6261	+61425	2058	21210	15645	+5565	-1735
2072	33221	21717	+11504	+72929	2059	8652	5463	+3189	+1454
2073	34330	24548	+9782	+82711	2060	8140	6032	+2108	+3562
2074	31809	25064	+6745	+89456	2061	10296	10435	-139	+3423
2075	22720	15991	+6729	+96185	2062	13137	9397	+3740	+7163
2076	16257	10427	+5830	+102015	2063	16525	13689	+2836	+9999
2077	21409	13839	+7570	+109585	2064	9525	6240	+3285	+13284
2078	15626	10267	+5359	+114944	2065	6088	3379	+2709	+15993
2079	14932	8967	+5965	+120909	2066	14759	10096	+4663	+20656
2080	3389	2981	+408	+121317	2067	8625	7149	+1476	+22132
2081	11025	9465	+1560	+122877	2068	10316	11273	-957	+21175
2082	7087	5952	+1135	+124012	2069	7131	5328	+1803	+22978
2083	10265	8997	+1268	+125280	2070	2233	2005	+228	+23206
2084	5720	4603	+1117	+126397	2071	8688	5910	+2778	+25984
2085	13717	10454	+3263	+129660	2072	20334	10254	+10080	+36064
2086	24433	18668	+5765	+135425	2073	5288	2714	+2574	+38638
2087	23862	15622	+8240	+143665	2074	10966	6430	+4536	+43174
2088	13365	7578	+5787	+149452	2075	21330	14283	+7047	+50221
2089	7972	4112	+3860	+153312	2076	13487	9114	+4373	+54594
Norikura									
2010	6295	3231	+3064	+3064	2077	—	—	—	+54594
2011	3218	1407	+1811	+4875	2078	3599	2052	+1547	+56141
2012	4390	1717	+2673	+7548	2079	1264	392	+872	+57013
2013	9621	6994	+2627	+10175	2080	6086	4361	+1725	+58738
2014	15286	7679	+7607	+17782	2081	1963	1294	+669	+59407
2015	7171	4435	+2736	+20518	2082	3958	3069	+889	+60296
2016	4266	2883	+1383	+21901	2083	4275	3675	+600	+60896
2017	18103	15449	+2654	+24555	2084	2588	2865	-277	+60619
2018	46959	34053	+12906	+37461	2085	—	—	—	+60619
2019	20278	18860	+1418	+38879	2086	—	—	—	+60619
2020	13045	10723	+2322	+41201	2087	—	—	—	+60619
2021	11570	17925	-6355	+34846	2088	—	—	—	+60619
2022	17172	27947	-10775	+24071	2089	2055	1483	+572	+61191
2023	7031	10406	-3375	+20696	Pic du Midi				
2024	12377	14332	-1955	+18741	2010	9046	6352	+2694	+2694
2025	—	—	—	+18741	2011	12707	8226	+4481	+7175
2026	7604	9845	-2241	+16500	2012	26257	16590	+9667	+16842
2027	19038	20226	-1188	+15312	2013	17574	12666	+4908	+21750
2028	11555	16706	-5151	+10161	2014	11601	8615	+2986	+24736
2029	7401	13091	-5687	+4474	2015	22771	14714	+8057	+32793
2030	4252	5125	-873	+3601	2016	16639	17315	-676	+32117
2031	5899	8884	-2985	+616	2017	24792	20236	+4556	+36673
2032	2713	5342	-2629	-2013	2018	38745	29026	+9719	+46392
2033	5388	6410	-1022	-3035	2019	31206	30897	+309	+46701
2034	20629	24208	-3579	-6614	2020	27309	22373	+4936	+51637
2035	34765	43507	-8742	-15356	2021	19245	17740	+1505	+53142
2036	19296	25212	-5916	-21272	2022	27192	32028	-4836	+48306
2037	5010	7305	-2295	-23567	2023	9325	11813	-2488	+45818
2038	2411	2115	+296	-23271	2024	24196	25804	-1608	+44210
2039	13868	13815	+53	-23218	2025	10432	14247	-3815	+40395
2040	8076	7507	+569	-22649	2026	16164	19903	-3739	+36656
2041	10332	7286	+3046	-19603	2027	16705	19749	-3044	+33612
2042	7454	5881	+1573	-18030	2028	10770	13742	-2972	+30640
					2029	10074	12184	-2110	+28530

Continuation Table XVII

Rot.	N	S	N—S	$\Sigma(N-S)$	Rot.	N	S	N—S	$\Sigma(N-S)$
2030	15156	17974	—2818	+25712	2018	10466	9377	+1089	+21308
2031	17011	24343	—7332	+18380	2019	19008	17341	+1667	+22975
2032	33050	39681	—6631	+11749	2020	20296	19105	+1191	+24166
2033	8634	13274	—4640	+7109	2021	30014	31791	—1777	+22389
2034	27286	28624	—1338	+5771	2022	23871	30092	—6221	+16168
2035	19382	20028	—646	+5125	2023	23168	29285	—6117	+10051
2036	27144	27370	—226	+4899	2024	10406	11231	—825	+9226
2037	23007	20600	+2407	+7306	2025	13496	21421	—7925	+1301
2038	19162	19845	—683	+6623	2026	13173	18315	—5142	—3841
2039	6908	6699	+209	+6832	2027	16682	21357	—4675	—8516
2040	4482	4439	+43	+6875	2028	14530	19726	—5196	—13712
2041	11856	8406	+3450	+10325	2029	23515	37967	—14452	+28164
2042	8765	7626	+1139	+11464	2030	2234	3264	—1030	+29194
2043	10648	7594	+3054	+14518	2031	—	—	—	+29194
2044	25899	16266	+9633	+24151	2032	—	—	—	+29194
2045	24261	20661	+3600	+27751	2033	—	—	—	+29194
2046	23493	20792	+2701	+30452	2034	—	—	—	+29194
2047	27058	23378	+3680	+34132	2035	—	—	—	+29194
2048	21197	19733	+1464	+35596	2036	—	—	—	+29194
2049	10134	10499	—365	+35231	2037	12405	11329	+1076	+28118
2050	6591	6040	+551	+35782	2038	11340	8854	+2486	+25632
2051	15782	15264	+518	+36300	2039	7598	8687	—1089	+26721
2052	23867	19933	+3934	+40234	2040	18099	15103	+2996	+23725
2053	15000	12643	+2357	+42591	2041	21364	18045	+3319	+20406
2054	12705	9891	+2814	+45405	2042	13832	10071	+3761	+16645
2055	12893	10311	+2582	+47987	2043	21749	16555	+5194	+11451
2056	20470	16029	+4441	+52428	2044	19906	13175	+6731	+4720
2057	21026	16679	+4347	+56775	2045	—	—	—	+4720
2058	23112	15690	+7422	+64197	2046	7380	6305	+1075	+3645
2059	9329	6285	+3044	+67241	2047	14632	13604	+1028	+2617
2060	4603	3594	+1009	+68250	2048	24447	24677	—230	+2847
2061	15763	11606	+4157	+72407	2049	10046	10254	—208	+3055
2062	15223	10814	+4409	+76816	2050	30222	27074	+3148	+93
2063	15086	7847	+7239	+84055	2051	20205	16992	+3213	+3306
2064	11601	6287	+5334	+89389	2052	27919	19776	+8143	+11449
2065	11704	7971	+3733	+93122	2053	12663	9188	+3475	+14924
2066	9891	7322	+2569	+95691	2054	18685	11457	+7228	+22152
2067	4583	3412	+1171	+96862	2055	18630	10606	+8024	+30176
2068	23449	15356	+8093	+104955	2056	18679	12013	+6666	+36842
2069	14260	9662	+4598	+109553	2057	8013	6213	+1800	+38642
2070	19655	14244	+5411	+114964	2058	10660	8099	+2561	+41203
2071	20028	12626	+7402	+122366	2059	9339	4585	+4754	+45957
2072	18332	10837	+7495	+129861	2060	33497	19131	+14366	+60323
2073	29139	19106	+10033	+139894	2061	4038	3095	+943	+61266
2074	7031	5383	+1648	+141542	2062	18373	13293	+5080	+66346
2075	6989	5333	+1656	+143198	2063	7129	4182	+2947	+69293
2076	6039	2769	+3270	+146468	2064	5092	3057	+2035	+71328
2077	—	—	—	+146468	2065	5697	3050	+2647	+73975
2078	4789	3971	+818	+147286	2066	4197	2076	+2121	+76096
2079	21625	15751	+5874	+153160	2067	3396	1852	+1544	+77640
2080	32088	23607	+8481	+161641	2068	—	—	—	+77640
2081	9079	8538	+541	+162182	2069	4520	3252	+1268	+78908
2082	7715	6286	+1429	+163611	2070	2865	1353	+1512	+80420
2083	13688	10466	+3222	+166833	2071	2174	1310	+864	+81284
2084	17797	12770	+5027	+171860	2072	4936	3120	+1816	+83100
2085	15011	11421	+3590	+175450	2073	6312	3933	+2379	+85479
2086	23988	19239	+4749	+180199	2074	9543	7110	+2433	+87912
2087	36378	18520	+17858	+198057	2075	7406	5031	+2375	+90287
2088	9211	5920	+3291	+201348	2076	3782	2399	+1383	+91670
2089	7971	4352	+3619	+204967	2077	5812	3151	+2661	+94331
Sacramento Peak					2078	774	424	+350	+94681
2010	8563	6779	+1784	+1784	2079	7031	4120	+2911	+97592
2011	3362	2358	+1004	+2788	2080	4995	3881	+1114	+98706
2012	11180	7595	+3585	+6373	2081	7560	6061	+1499	+100205
2013	14686	8145	+6541	+12914	2082	3776	2973	+803	+101008
2014	16541	11680	+4861	+17775	2083	3148	1836	+1312	+102320
2015	12181	9438	+2743	+20518	2084	1114	429	+685	+103005
2016	2453	2625	—172	+20346	2085	4210	2530	+1680	+104685
2017	3648	3775	—127	+20219	2086	3018	1907	+1111	+105796
					2087	2673	1589	+1084	+106880
					2088	2934	1365	+1569	+108449
					2089	3133	1507	+1626	+110075

Continuation Table XVII

Wendelstein

Rot.	N	S	N — S	$\Sigma(N - S)$	Rot.	N	S	N — S	$\Sigma(N - S)$
2010	3028	1230	+1798	+1798	2050	8025	7536	+489	-5585
2011	602	357	+245	+2043	2051	6908	6043	+865	-4720
2012	3093	2051	+1042	+3085	2052	21731	18041	+3690	-1030
2013	3704	1415	+2289	+5374	2053	10518	8624	+1894	+864
2014	1380	933	+447	+5821	2054	9402	7769	+1633	+2497
2015	4742	3350	+1392	+7213	2055	7119	4973	+2146	+4643
2016	1709	1712	-3	+7210	2056	4191	3283	+908	+5551
2017	7895	8251	-356	+6854	2057	8591	7016	+1575	+7126
2018	8843	7884	+959	+7813	2058	6675	5808	+867	+7993
2019	8271	7465	+806	+8619	2059	15755	12099	+3656	+11649
2020	13687	12291	+1396	+10015	2060	14873	12101	+2772	+14421
2021	8892	7781	+1111	+11126	2061	14379	12733	+1646	+16067
2022	7748	8751	-1003	+10123	2062	7671	5933	+1738	+17805
2023	5740	7541	-1801	+8322	2063	8986	6908	+2078	+19883
2024	9084	11241	-2157	+6165	2064	3910	2182	+1728	+21611
2025	5342	7271	-1929	+4236	2065	8281	4915	+3366	+24977
2026	7372	9485	-2113	+2123	2066	3800	2333	+1467	+26444
2027	6422	8321	-1899	+224	2067	7094	4720	+2374	+28818
2028	4331	5781	-1450	-1226	2068	2799	2221	+578	+29396
2029	6741	9352	-2611	-3837	2069	7774	5479	+2295	+31691
2030	8292	11581	-3289	-7126	2070	5885	3687	+2198	+33889
2031	4525	6531	-2006	-9132	2071	1903	1559	+344	+34233
2032	3201	4606	-1405	-10537	2072	5025	3114	+1911	+36144
2033	5826	8383	-2557	-13094	2073	10204	6756	+3448	+39592
2034	18062	22305	-4243	-17337	2074	8663	6227	+2436	+42028
2035	14341	15366	-1025	-18362	2075	5448	3657	+1791	+43819
2036	7291	7612	-321	-18683	2076	4618	2868	+1750	+44569
2037	4884	4717	+167	-18516	2077	4505	2550	+1955	+47524
2038	5924	5269	+655	-17861	2078	6169	3996	+2173	+49697
2039	1988	1695	+293	-17568	2079	7331	3809	+3522	+53219
2040	5937	5105	+832	-16736	2080	3808	2313	+1495	+54714
2041	5839	4285	+1554	-15182	2081	4953	3391	+1562	+56276
2042	3108	2632	+476	-14706	2082	431	358	+73	+56349
2043	5626	4637	+989	-13717	2083	2226	1246	+980	+57329
2044	13446	10389	+3057	-10660	2084	6561	3931	+2630	+59959
2045	14428	12186	+2242	-8418	2085	5880	3412	+2468	+62427
2046	12836	11476	+1360	-7058	2086	7841	5298	+2543	+64970
2047	5169	5002	+167	-6891	2087	6665	3546	+3119	+68089
2048	10840	10343	+497	-6394	2088	8305	3730	+4575	+72664
2049	10553	10233	+320	-6074	2089	8011	4096	+3915	+76579

Table XVIII
Total and relative N — S asymmetry of the corona from 1956 till 1961

Station	N	S	N + S	N — S	$\frac{N - S}{N + S} \%$
Arosa	179816	159362	339178	+20454	+6.03
Climax	1637346	1451553	308899	+185793	+6.01
Kanzelhöhe	379927	363546	743473	+16381	+2.20
Kislovodsk	1139701	986389	2126090	+153312	+7.21
Norikura	749688	688497	1438185	+61191	+4.25
Pic du Midi	1340774	1135807	2476581	+204967	+8.28
Sacr. Peak	824421	714346	1538767	+110075	+7.15
Wendelstein	573656	497077	1070733	+76579	+7.15

southern hemisphere, the northern hemisphere prevailed also in the corona, except for 1957. The same applies to the chromospheric flares of this period (QBSA).

Table XVIII gives the final total and relative N — S asymmetry.

From our numerical results we may conclude as follows:

North-South asymmetry in the corona was found by all stations and is, thus, real and consistent with the asymmetry in other phenomena on the Sun. Except for Kanzelhöhe, the asymmetry value of all stations is very much the same and so high that measuring errors do not mask it. The N — S asymmetry for Norikura and especially for Kanzelhöhe was brought down by instru-

mental errors in favour of the southern hemisphere.

The effects of the first- and second-type errors, that is of errors due to observational method and to atmospheric conditions, markedly differ, according to whether they show in the N — S or E — W asymmetry. This can be explained as follows: In the N — E — S — W — N measuring system, the western always succeed the eastern quadrants, while the northern and southern quadrants alternate. In the former case, therefore, the errors cumulate, while they get compensated in the latter case, and are then distributed almost uniformly over the northern and southern hemisphere.

E — W and N — S asymmetry as compared to the asymmetry in other phenomena on the Sun

The coronal N — S asymmetry was for all stations governed by the northern hemisphere from 1956 till 1961, except for the year 1957. The N — S asymmetry in the number of spot groups was almost the same (Astronomische Mitteilungen der Eidgenössischen Sternwarte, Zürich). The prominence-profile areas, as given in the same source, were governed by the northern hemisphere all through the years in question. The northern hemisphere also prevailed in chromospheric flares until the end of the investigated period, except for the years 1956 till 1958 (QBSA). However, the predominance of the southern hemisphere having been insignificant in comparison to that of the northern hemisphere, the total asymmetry was also positive for chromospheric flares.

Thus, the corona is not an exception in the N — S asymmetry: its asymmetry is consistent with that of the other solar phenomena mentioned.

The E — W asymmetry in spots and chromospheric flares for the same period is as follows:

The number of the spot groups on the eastern and western half of the solar disc was determined from the Heliographische Karten der Photosphäre

Table XX

Phenomen	E — W	$\frac{E - W}{E + W}$
Spot groups	—381	—1.36 %
Chromospheric flares	—136	—0.85

by adding up all groups that had passed through the individual diurnal segments of the disc.

If we ventured a parallel to the N — S asymmetry, then, if the E — W asymmetry in spots and chromospheric flares (the material on prominences was not processed) is not positive it should not be positive in the corona either.

Conclusions

From the results and considerations in the preceding sections, we may conclude as follows:

1. Measurements made at 9 coronal stations show that the North-South asymmetry of the solar corona is real and that it agrees with the asymmetry of other phenomena on the Sun (sunspots, prominences, chromospheric flares). The corona is, thus, included in the general problem of the relative activity of the northern and southern solar hemisphere.

2. The results on the East-West asymmetry, arrived at from observations made by different stations, but based on the same material as the investigation into the North-South asymmetry, are antagonistic throughout. There is no factual evidence to bear out the positive asymmetry as derived by Link and Linková for a shorter period. For the only station with systematic positive asymmetry, that on Pic du Midi, we have just proved measuring errors. Hence follows that insofar as there does exist an E — W asymmetry in the corona, it is insignificant and overlapped by larger observational errors.

3. The systematic errors at some observing stations are rather great and chiefly due to varying atmospheric conditions in combination with the incorrect observational method. The predominance of cases with conditions getting poorer as the observations along the solar limb wear on, leads to a systematic error in the measured intensity, dependent on the position angle. The measurements also betray systematic errors of instrumental origin that may amplify the previous errors (Pic du Midi) or overlap them throughout (Nori-kura).

4. The method of publishing the results in the

Table XIX

Phenomen	N — S	$\frac{N - S}{N + S}$
Spot groups	+642	+14.05 %
Chromospheric flares	+427	+17.12
Prominences	+1560	+8.24
Corona (average of all stations)		+6.1

QBSA used so far is unsatisfactory in that Pic du Midi does not distinguish between cases, where the intensity of the corona was zero at a certain position angle, and cases, where no measurements were made at the given angle. Data on atmospheric conditions and on their variations are not to be got at all.

5. In order to improve the quality of corona-intensity measurements and of the results derived from them, the following is recommended:

a) Instrumental errors should be suppressed as much as possible by minutely centring all optical elements and diaphragms of the coronograph. Greatest attention should be paid to the maintenance of the coronograph axis in the direction to the centre of the solar disc.

b) More attention should be paid to the varia-

bility of atmospheric conditions throughout every observation. The respective data on the quality of the conditions together with the results should be published.

c) The corona measurements should be calibrated by check-up measurements at the end of every series; this should be done above the region without any active centre at as short intervals as possible from the first measurements.

d) The minimum requirement for a homogenization of the material without calibration is to alternate the position angle of the beginning of the observation, such as S, W, N, E, S, . . . , which would uniformly distribute all over the four quadrants the errors due to atmospheric effects and to the adaptation and fatigue of the eye.

REFERENCES

- Bouška J., 1951, CR Paris 232, 1643.
Brunner-Hogger W., 1939, Astr. Mitt. Zürich, No. 137.
Bruzek A., 1954, ZFA 33, 267.
Gleissberg W., 1947, Observatory 67.
Gnevyshev M. N., 1963, Astr. žurnal 51, 401.
Kopecký M., Mayer P., 1951, BAC 2.
Kopecký M., Mayer P., Borovičková V., 1952, BAC 3, 37.
Kulešová K. F., 1963, Solnečnye dannye, No. 9, 10, 11.
Kulešová K. F., Slonim J. M., 1957, Solnečnye dannye, No 3.
Link F., 1964, BAC 15, 187.
Link F., Linková Z., 1957, BAC 8, 79.
Maunder A. S. D., 1907, MN 67, 451.
Pajdušáková L., 1958, BAC 9, 201.
Pocok R. J., 1919, MN 79, 54.
Waldmeier M., 1935, Astr. Mitt. Zürich No. 133.
Waldmeier M., 1955, Ergebnisse und Probleme der Sonnenforschung (Leipzig), 284.

Л. ПАЙДУШАКОВА

АСИММЕТРИЯ СОЛНЕЧНОЙ КОРОНЫ

Северо-южная относительно экватора асимметрия солнечной активности доказана уже раньше. Эта асимметрия была найдена также для интенсивности солнечной короны. Семь из девяти корональных станций обнаруживают асимметрию $A = \frac{C - Ю}{C + Ю}$ больше чем + 6%, наиболее высокая у станции Пик дю Миди (+8,2%). Для станций Канцельгоге (+2,2%) и Норикуры (+4,2%) С—Ю асимметрия понижена влиянием ошибок прибора.

В предложенной работе исследуется в первую очередь восточно-западная асимметрия солнечной короны на основании материала, опубликованного корональными станциями в QBSA,. В период 1948—1961 гг. полная асимметрия (В — З) оказалась у четырех станций положительной, у пяти отрицательной. Кривые кумулятивных сумм (В — З) не показывают общую зависимость, во всяком периоде станции обнаруживают поочередно положительную и отрицательную асимметрии. Только станция Пик дю Миди обнаруживает в течение всего исследуемого периода положительную асимметрию. На основании этого результата можно сделать заключение с двумя альтернативами: 1. существует восточно-западная асимметрия, как ее показывает станция Пик дю Миди, и в этом случае значения асимметрии всех остальных станций отяготены ошибками; 2. результаты станции Пик дю Миди тоже отягощены систематическими ошибками, предполагающими восточную сторону солнечного диска. Во всяком случае можно заключить, что восточно-западная асимметрия меньше ошибок наблюдений, если она вообще существует.

Возможные ошибки, оказывающие влияние на результаты измерений интенсивности солнечной короны, скорее всего можно обнаружить у станции Пик дю Миди, так как в соответствии с второй альтернативой они являются систематическими и постоянными.

Обсуждаются следующие типы ошибок:

1. Ошибки, вызванные методикой наблюдений. Если существуют изменяющиеся в течение одного наблюдения солнечной короны условия (напр. атмосферные условия, адаптация и усталость глаза) и наблюдения проводятся всегда с одной и, той-же точки солнечного диска и в том-же направлении, происходит накопление ошибок только в определенных квадрантах. Показано, что у станции Пик дю Миди происходит такое накопление ошибок вследствие изменяющихся атмосферных условий, понижающих данные последних измеренных квадрантов.

2. В течение измерения вдоль края всего солнечного диска, может произойти изменение атмосферных условий, с наибольшей вероятностью их ухудшение, потому что наблюдения начинаются, как правило, только при „корональных условиях“. Эта ошибка очень выразительно выступает в материале станции Пик дю Миди, в котором стремительно возрастает число квадрантов без измерений в применяемом направлении измерений С — В — Ю — З — С. Чтобы избежать этой независимой от наблюдателя ошибки, нужно вести наблюдения, начиная поочередно всегда с другой точки солнечного диска, напр. с очередным изменением начальной точки С, В, Ю, З, С, и т. д.

3. Нет основания предполагать реальность

противоположного положения квадрантов с максимальным и минимальным значениями интенсивности, особенно если это положение для материала других станций оказывается прямо обратным, и если при изменении квадранта максимума изменяется также квадрант минимума. У станции Пик дю Миди этот факт — максимум в первом или втором квадрантах, минимум в третьем или четвертом квадрантах — можно объяснить только ошибкой прибора. Эта ошибка приборов у разных станций повидимому различна, и может вызвать положительную или-же отрицательную асимметрию (станция

Норикура). Только эта ошибка объясняет лишенные временной связи изменения положительной асимметрии в отрицательную у большинства станций.

Анализ ошибок измерений короны предъявляет следующие требования:

1. Атмосферные условия должно определять в начале и в конце наблюдений.
2. На всех станциях ввести общее обозначение для случаев неопределенной интенсивности короны.
3. Измерения производить, начиная поочередно с разных точек солнечного диска.

L. PAJDUSÁKOVÁ

ASYMETRIA SLNEČNEJ KORÓNY

Severojužná asymetria slnečnej činnosti voči rovníku je dokázaná už dávnejšie. Túto asymetriu N — S ukazuje i intenzita koróny. Z deviatich korónových staníc sedem vykazuje asymetriu $A = \frac{N - S}{N + S}$ viac ako + 6 %, najvyššiu Pic du Midi + 8,2 %. U stanice Kanzelhöhe (+ 2,2 %) a Norikury (+ 4,2 %) asymetriu N — S pravdepodobne znížila prístrojová chyba.

Predložená práca je venovaná predovšetkým východozápadnej asymetrii koróny, skúmanej na základe materiálu uverejňovaného korónovými stanicami v QBSA. Od roku 1948 do roku 1961 totálna asymetria (E — W) je u štyroch staníc kladná a u piatich záporná. Medzi krivkami kumulatívnych súťotov (E — W) nemožno nájsť jednotnú závislosť, v každom časovom úseku vykazujú stanice striedavo kladnú i zápornú asymetriu. Len stanica Pic du Midi vykazuje počas celého vyšetrovaného obdobia kladnú asymetriu. Z tohto výsledku možno urobiť záver o dvoch alternatívach: bud' asymetria E — W existuje, tak ako ukazuje Pic du Midi, a potom ostatné stanice sú zatažené chybami, alebo Pic du Midi je zatažené systematickou chybou v prospech východného okraja. V každom prípade však možno usúdiť, že asymetria E — W — ak vôbec existuje — je menšia ako pozorovacie chyby.

Možné chyby ovplyvňujúce výsledky merania intenzity koróny najskôr možno zistíť u Pic du Midi, pretože podľa nášho druhého predpokladu sú systematické a nemeniac sa.

Možno uvažovať o nasledujúcich typoch chýb:

1. Chyby vyplývajúce z metodiky pozorovania.

Ak pri pozorovaní koróny existujú podmienky, ktoré sa časom v priebehu jedného pozorovania menia a tým ovplyvňujú výsledok (napríklad atmosferické podmienky, adaptácia a únava oka), potom v prípade, že pozorovanie sa vždy začína od jedného bodu slnečného kotúča a pokračuje vždy tým istým smerom, chyby sa kumulujú v určitých kvadrantoch. U Pic du Midi sa dokázalo, že touto metódou sa kumuluje chyba vznikajúca zmenami atmosferických podmienok, a to v neprospech posledných meraných kvadrantov.

2. Za dobu potrebnú na premeranie celého okraju slnečného disku atmosferické podmienky sa môžu zmeniť, a to pravdepodobnejšie k horšiemu, keďže sa spravidla koróna začína pozorovať len za „korónových podmienok“. Túto chybu možno veľmi markantne ukázať na materiáli z Pic du Midi, kde rapídne vzrástá počet kvadrantov bez merania v smere zaužívaného postupu merania N — E — S — W — N. Túto chybu, nezávislú od pozorovateľa, možno štatisticky eliminovať tým, že pozorovanie sa striedavo začína vždy od iného bodu slnečného disku, napríklad s pravidelným striedením počiatočného bodu: N, E, S, W, N atď.

3. Neexistuje dôvod predpokladať reálnosť systematicky protiľahlého postavenia kvadrantov s maximálnou a minimálnou hodnotou intenzít, najmä ak iné stanice majú postavenie práve opačné, a ak sa zmenou kvadrantu maxima mení i kvadrant minima. Túto skutočnosť u Pic du Midi — maximum v prvom alebo v druhom kvadrante, minimum v tretom alebo štvrtom kvadrante — možno vysvetliť len prístrojovou chybou. Prístrojová chyba je pochopiteľne indi-

viduálna u každej stanice a môže viesť ako k asymetrii kladnej, tak i zápornej, ako je u stanice Norikury. Len touto chybou možno vysvetliť prechody asymetrie kladnej v zápornú u väčšiny staníc, a to bez časového súhlasu.

Z rozboru chýb meraní koróny vyplývajú požiadavky:

1. Ohodnocovať atmosferické podmienky na počiatku a konci pozorovania.
2. Na všetkých stanicach zaviesť jednotné označovanie pre prípady neurčenej intenzity koróny.
3. Merania začínať striedavo od rôznych bodov slnečného kotúča.